The Small World of Global Marine Fisheries: The Cross-Boundary Consequences of Larval Dispersal

One-sentence summary: Marine fisheries are internationally connected in a small-world network through larval dispersal, producing hotspots of risk.

Nandini Ramesh,[1*], James A. Rising,[2] Kimberly L. Oremus[3]

[1]Department of Earth and Planetary Science, University of California, Berkeley, Berkeley, CA 94720, USA

[2]Grantham Research Institute, London School of Economics, London, UK

[3]School of Marine Science and Policy, University of Delaware, Newark, DE, 19716, USA

[*]To whom correspondence should be addressed; E-mail: nandiniramesh@berkeley.edu.

Fish stocks are managed within national boundaries and by regional organizations, but the interdependence of stocks between these jurisdictions remains poorly explored, especially as a result of larval dispersal (*1, 2*). We examine the international connectivity of 747 **commercially fished taxonomic groups by building a global network of fish larval dispersal. We find that the world's fisheries are highly interconnected, forming a small-world network (*3*), highlighting the need for international cooperation. We quantify each country's dependence on its neighbors in terms of landed value, food security, and jobs. We estimate that over $10 billion in annual catch from 2005 – 2014 is attributable to these international flows of larvae. The economic risks associated with these dependencies is greatest in the Tropics.**

Marine fisheries supply food and livelihoods to millions of people around the world (*4*). Though fisheries are typically managed at the scale of national Exclusive Economic Zones (EEZs), many fish populations are connected beyond EEZ boundaries (*5–9*). While pelagic species can be tracked across international borders as adults (*10*), non-pelagic populations connect primarily via the dispersal of fish eggs and larvae that cannot yet swim by ocean currents (*5, 11*). Larval connectivity patterns have been analyzed at both the regional (*2, 9, 12–14*) and global levels (*7, 15, 16*), and have been used to suggest changes in spatial management and conservation (*14, 17*). However, the impact on fisheries of larval connectivity across EEZs is not well-understood, even though over 90% of the world's fish are caught within EEZs (*18*).

On the scale of a single species or region, this connectivity can be analyzed empirically through genetic testing (*12, 13*). For analyses on larger scales, dispersal patterns can be estimated using biophysical models that combine oceanographic data with an understanding of the stocks' biology (*7, 16*). One challenge is that species vary widely in larval timing and duration, and currents vary with the seasons, so generalizations can be misleading. More realistic inputs can be achieved by using life history traits for each species, including time and place of spawning and larval duration. Sensitivity analyses can help to ensure that results are robust to changes in key assumptions (*16*), while empirical bounding can safeguard against predicting unrealistic dispersion outcomes (*9*).

Network analysis has previously been applied to marine systems to describe the connectivity of plankton communities (*19*), local fishing communities (*20, 21*) and marine reserves (*16*). Networks of larval flows have been used to identify "hub" subpopulations for protection at a regional scale (*14*).

In this study, we combined oceanographic and life history data for 706 species and 434 genera of commercially harvested fish to estimate their connectivity across 249 EEZs and construct a network representing the larval flows between nations. Nations that depend heavily upon their neighbors for recruitment risk losing part of their catch if the fisheries in the source EEZs, which are outside their jurisdiction, are poorly managed. We quantified these risks in economic terms and identified regional "hotspots" of risk for catch, fishery employment, and food security.

We used a particle-tracking system (*22*) with time-varying ocean currents (*23*) and species-specific life histories (*24*) to simulate the dispersal of eggs and larvae through a dynamic ocean. We placed multiple simulated particles for each species based on the timing and location of that species' spawning, and let them drift for their larval duration to obtain a probabilistic estimate of species-specific larval trajectories. We used a random-walk parameterization (*22*) that adds a small velocity at every time step to account for turbulent motion at small scales (see SM 3.1.2).

We empirically bounded our results by discarding particles that arrive in regions where the species is not present in observed catch data (*18*). For a given EEZ, catch is attributed based on the proportion of particles arriving there from each spawning country (see SM 1.1). This proportionality forms the core assumption of our model. We test our main results with a series of sensitivity analyses to this assumption. These include reducing spawn floating duration to account for uncertainties in spawning mortality (*5, 25*), introducing return adult spawning migration (*26*) (see SM 3.6), and distinguishing different levels of recruitment limitation.

We estimate how much of each country's observed catch comes from its neighbors by constructing for each species a transition matrix that describes the probability of its offspring dispersing from one EEZ to another. This transfer of biomass between nations' EEZs is represented as a network in Fig. 1.

Each connector of the network represents net flows of fish from one country to another. Coun-

Fig. 1 goes near here.

tries that depend on inflows of juvenile fish to maintain their local populations require international cooperation to ensure sustainable fisheries. Our analysis of these flows reveals that a large proportion of marine fisheries within EEZs form a single, global network (Fig. 1).

We find that the global network of marine fisheries is a scale-free, small-world network. The scale-free network property, common in natural systems (*3*), is characterized by an exponential distribution of the number of connections from each node (see SM 3.2). This exponential degree distribution results in a "hub-and-spoke" structure that is resilient to random disturbances because of the large number of less-connected countries from which disturbances do not easily propagate to other parts of the network. However, a disturbance to any of the highly-connected hubs in a scale-free network can affect numerous surrounding nodes. In this context, this suggests that habitat destruction, overfishing, or environmental change in a hub EEZ could have impacts that spread beyond its own boundaries. Conversely, targeted efforts to manage fisheries within these hub EEZs could benefit many nations.

To demonstrate the relationship between currents and the network of larval dispersal, we zoom in on four regions (Fig. 2). The differences between the regional networks and average current speed arise from the details of current speeds during spawning, larval duration, and empirical observations of species presence or catch. The influence of the Guinea Current on the connectivity of West Africa's fisheries can be seen in the large number of EEZs that act as sources to their eastward neighbors, especially between Guinea-Bissau and Nigeria. While the strongest connections are typically between adjacent EEZs, many connections also extend over longer distances. In contrast, the Baltic Sea has significantly weaker currents. Here, the largest outward flows originate from Sweden and Norway, which have the region's longest coastlines. In the

Caribbean, the North Brazil Current flows northwestward along the South American coast, and consequently many of the EEZs lying along this current act as sources for the Lesser Antilles. Within the Lesser Antilles, the density of small EEZs gives rise to a highly-interconnected, complex network structure. The effect of the northward flow along this island chain can be inferred from the larger node sizes among the EEZs lying in its southern portion. In the Western Pacific, strong currents dominate in the equatorial ocean, with weaker currents at higher latitudes. The large areas encompassed by this region's EEZs mean that, unlike the other regions, most connections are between immediate neighbors.

Fig. 2 goes near here.

The small-world property implies that it is possible to traverse the global network in a small number of steps, on average. Within this network, there exist smaller clusters or communities that are tightly connected. Most of these clusters internally exhibit the small-world property. In theory, this property of the global fisheries network suggests that disturbances to a large hub could propagate via cascading effects on the surrounding spokes.

A key question is whether disruptions to a given EEZ actually propagate in this manner. A stock's response to external shocks depends on both its population dynamics and mortality from fishing, which can be affected by management (*27*). Some fish stocks are biologically capable of replenishing themselves when their numbers dwindle, provided fishing pressure is relieved, reducing the likelihood that disturbances will propagate. However, "recruitment-limited" stocks are vulnerable to a decline in spawning population, making it more likely that disturbances will spread across the network even if the receiving fisheries are managed. We adopted Fishbase's classification of stock resilience as a proxy for this type of density dependence. For high-resilience stocks, which are generally not recruitment-limited, our measure of stock dependence overestimates the extent to which stocks will be reduced if recruitment inflows fail. For those classified as medium- and low-resilience, however, we found a strong correlation between our simulation's predictions and observed variance in stock levels (see SM 3.5). Even for countries whose fisheries mostly comprise non-density-dependent stocks, these larval inflows serve as a buffer against fishery collapse within their waters.

To contextualize our results, we estimated the economic significance of the network's international connections. First, we considered the amount and value of catch that flows in and out of each EEZ (see Fig. 3). Japan, China, and Alaska are responsible for the greatest outflows, reflecting their productive waters. However, having fewer neighbors makes them smaller hubs (see Fig. 1). Indonesia has the most landed value attributable to other countries, due to its high-value catch and many neighbors. The countries with the greatest catch inflows are generally those with the largest fisheries. Next, we identified nations that are potentially most vulnerable

Fig. 3 goes near here.

to the management of neighboring waters in socioeconomic terms (see table S5). In Fig. 4, we highlight countries that depend the most on the spawning grounds of neighbors in terms of their total catch, GDP, jobs in the fishery industry, and a fishery food security dependence index (*28*). The most vulnerable nations are concentrated in the "hotspot" regions of the Caribbean, West Africa, Northern Europe, and Oceania. The risks to national GDP and labor force are generally highest in the Tropics. However, our measure of food-security risk also identified a few European nations.

Fig. 4 goes near here.

Our analysis shows that about 10 billion USD worth of annual marine catch may rely on transnational exchanges of fish offspring. These dependencies form a single global network, indicating that marine fisheries, even within national boundaries, constitute an interconnected, globally shared resource.

This network's scale-free and small-world properties imply that fish stocks from a small number of EEZs provide benefits to a large number of "downstream" countries. The most vulnerable nations are clustered in a few "hotspot" regions (Fig. 4). This pattern lends further support to the use of international frameworks such as Large Marine Ecosystems and Marine Protected Area networks (*29, 30*).

Further research is needed to understand how small-scale coastal processes, larval behaviour, and fisheries management impact this connectivity. Beyond the spawning connections studied here, national fisheries are interdependent through the movement of adult fish, population shifts under climate change, and international fishing treaties. In particular, the role of adult fish migration in driving international connectivity remains an important question. While a more detailed analysis is required to accurately describe dispersal pathways of individual species, this study highlights the role of larval connectivity across international boundaries and the need for multilateral cooperation for sustainable management of these shared resources.

References

1. M. J. Fogarty, L. W. Botsford, *Oceanography* **20**, 112 (2007).
2. M. Dubois, *et al.*, *Global ecology and biogeography* **25**, 503 (2016).
3. D. J. Watts, S. H. Strogatz, *Nature* **393**, 440 (1998).
4. FAO, *The state of world fisheries and aquaculture* (2016).
5. R. K. Cowen, S. Sponaugle, *Annual Review of Marine Science* (2009).

6. A. Di Franco, *et al.*, *Biol. Conserv.* **192**, 361 (2015).

7. E. Popova, *et al.*, *Mar. Policy* **104**, 90 (2019).

8. B. P. Kinlan, S. D. Gaines, *Ecology* **84**, 2007 (2003).

9. A. S. Kough, C. B. Paris, M. J. Butler, IV, *PLoS One* **8** (2013).

10. B. A. Block, *et al.*, *Nature* **434**, 1121 (2005).

11. D. A. Siegel, *et al.*, *Proceedings of the National Academy of Sciences* **105**, 8974 (2008).

12. S. Planes, G. P. Jones, S. R. Thorrold, *Proceedings of the National Academy of Sciences* **106**, 5693 (2009).

13. N. K. Truelove, *et al.*, *Fisheries Research* **172**, 44 (2015).

14. J. R. Watson, *et al.*, *Proceedings of the National Academy of Sciences* **108**, E907 (2011).

15. S. Wood, C. B. Paris, A. Ridgwell, E. J. Hendy, *Glob. Ecol. Biogeogr.* **23**, 1 (2014).

16. M. Andrello, *et al.*, *Nat. Commun.* **8**, 16039 (2017).

17. S. D. Gaines, C. White, M. H. Carr, S. R. Palumbi, *Proceedings of the National Academy of Sciences* **107**, 18286 (2010).

18. D. Pauly, D. Zeller, eds., *Sea Around Us Concepts, Design and Data* (University of British Columbia, 2015).

19. B. F. Jönsson, J. R. Watson, *Nat. Commun.* **7**, 11239 (2016).

20. E. C. Fuller, J. F. Samhouri, J. S. Stoll, S. A. Levin, J. R. Watson, *ICES J. Mar. Sci.* **74**, 2087 (2017).

21. E. T. Addicott, *et al.*, *Can. J. Fish. Aquat. Sci.* **76**, 56 (2019).

22. C. B. Paris, J. Helgers, E. van Sebille, A. Srinivasan, *Environmental Modelling & Software* **42**, 47 (2013).

23. J. A. Carton, B. S. Giese, *Monthly Weather Review* **136**, 2999 (2008).

24. R. Froese, D. Pauly, Fishbase (2014). World Wide Web electronic publication, version 11/2014.

25. C. C. D'Aloia, *et al.*, *Proceedings of the National Academy of Sciences* **112**, 13940 (2015).

26. A. Hastings, L. W. Botsford, *Proc. Natl. Acad. Sci. U. S. A.* **103**, 6067 (2006).

27. D. Pauly, *et al.*, *Nature* **418**, 689 (2002).

28. M. Barange, *et al.*, *Nature Clim. Change* **4**, 211 (2014).

29. B. S. Halpern, S. E. Lester, K. L. McLeod, *Proc. Natl. Acad. Sci. U. S. A.* **107**, 18312 (2010).

30. J. Lubchenco, *Stress, Sustainability, and Development of Large Marine Ecosystems during Climate Change: Policy and Implementation* (UNDP and GEF, 2013).

31. SCRFA, Fish aggregation database (2017).

32. D. Pauly, D. Zeller, eds., *Catch Reconstruction: concepts, methods and data sources* (University of British Columbia, 2015). Online Publication. Sea Around Us (www.seaaroundus.org).

33. B. S. Miller, A. W. Kendall, *Early Life History of Marine Fishes* (University of California Press, 2009), pp. 9–38.

34. K. Kaschner, *et al.*, Aquamaps: Predicted range maps for aquatic species (2012). World wide web electronic publication, version 08/2013.

35. R. P. Abernathey, J. Marshall, *Journal of Geophysical Research: Oceans* **118**, 901 (2013).

36. M. D. Humphries, K. Gurney, *PLoS One* **3**, e0002051 (2008).

37. M. Bolanos, E. M. Bernat, B. He, S. Aviyente, *Journal of neuroscience methods* **212**, 133 (2013).

38. J.-P. Onnela, J. Saramäki, J. Kertész, K. Kaski, *Physical Review E* **71**, 065103 (2005).

39. V. D. Blondel, J.-L. Guillaume, R. Lambiotte, É. Lefebvre, *J of Statistical Mechanics: Theory and Experiment* **10**, P10008 (2011).

40. L. C. Teh, U. R. Sumaila, *Fish and Fisheries* **14**, 77 (2013).

41. J. Murray, B. J, Composition of fish, *Tech. rep.*, Ministry of Technology, Torry Research Station (2001).

42. S. C. Walpole, *et al.*, *BMC Public Health* **12**, 439 (2012).

43. ram legacy stock assessment database (2018). Version 4.44-assessment-only. Released 2018-12-22. Retrieved from DOI:10.5281/zenodo.2542919.

Acknowledgments The authors thank Denyse Dookie, Matt Burgess, Mark A. Cane, Augustin Chaintreau, Aaron Carlisle, Jonathan Cohen, Chris Costello, Ruth Defries, Steve Gaines, Solomon Hsiang, Carlos Moffat, and Cody Szuwalski for comments, suggestions, and references. The authors declare they have no competing financial interests. N.R. performed the network analysis and Lagrangian modeling. J.A.R performed the country-level risk analysis. N.R., J.A.R. and K.L.O. designed the study, collected data and wrote the paper. All newly organized data used in this study and the intermediate and final results data are publicly available at `https://zenodo.org/record/2636745`. Analysis reproduction code is available at

https://github.com/openmodels/small-world-fisheries.

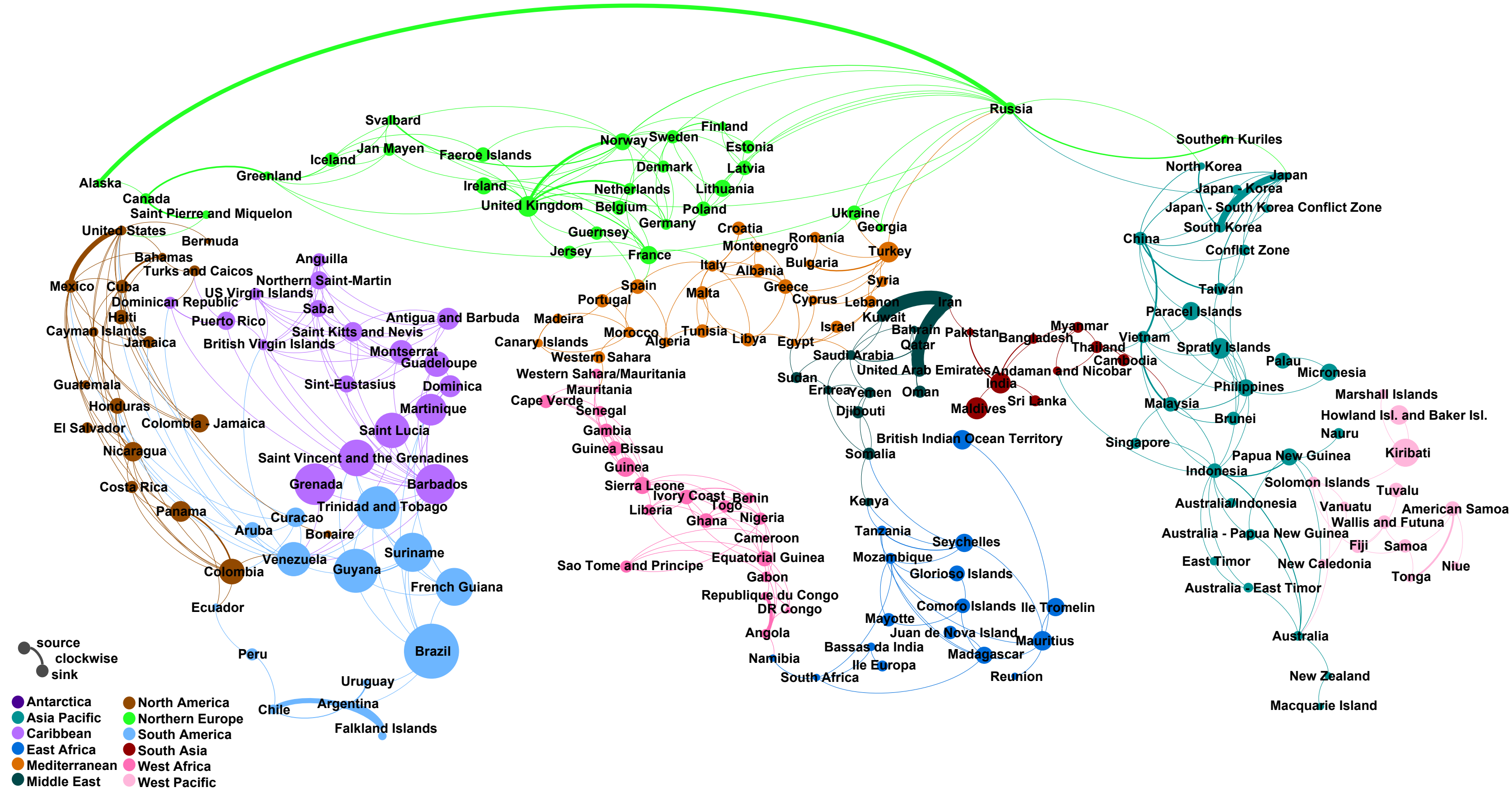

Russia
Svalbard
Jan Mayen
Iceland
Faeroe Islands
Norway
Sweden
Finland
Estonia
Latvia
Lithuania
Denmark
Netherlands
Belgium
Poland
Germany
Ireland
United Kingdom
Guernsey
Jersey
France
Alaska
Canada
Greenland
Saint Pierre and Miquelon
United States
Bermuda
Bahamas
Turks and Caicos
Mexico
Cuba
Dominican Republic
Haiti
Cayman Islands
Jamaica
Guatemala
Honduras
El Salvador
Colombia - Jamaica
Nicaragua
Costa Rica
Panama
Colombia
Ecuador
Peru
Chile
Argentina
Uruguay
Falkland Islands
Brazil
Anguilla
Northern Saint-Martin
US Virgin Islands
Saba
Puerto Rico
Antigua and Barbuda
Saint Kitts and Nevis
British Virgin Islands
Montserrat
Guadeloupe
Sint-Eustasius
Dominica
Martinique
Saint Lucia
Saint Vincent and the Grenadines
Grenada
Barbados
Trinidad and Tobago
Curacao
Aruba
Bonaire
Venezuela
Guyana
Suriname
French Guiana
Ukraine
Georgia
Croatia
Romania
Montenegro
Turkey
Italy
Albania
Bulgaria
Spain
Portugal
Malta
Greece
Syria
Cyprus
Lebanon
Madeira
Morocco
Algeria
Tunisia
Libya
Israel
Egypt
Canary Islands
Western Sahara
Western Sahara/Mauritania
Mauritania
Cape Verde
Senegal
Gambia
Guinea Bissau
Guinea
Sierra Leone
Ivory Coast
Benin
Togo
Liberia
Ghana
Nigeria
Cameroon
Sao Tome and Principe
Equatorial Guinea
Gabon
Republique du Congo
DR Congo
Angola
Namibia
South Africa
Iran
Kuwait
Bahrain
Qatar
Saudi Arabia
United Arab Emirates
Sudan
Eritrea
Yemen
Oman
Djibouti
Somalia
Pakistan
Bangladesh
Myanmar
Thailand
Cambodia
Andaman and Nicobar
India
Maldives
Sri Lanka
British Indian Ocean Territory
Kenya
Tanzania
Seychelles
Mozambique
Glorioso Islands
Comoro Islands
Ile Tromelin
Mayotte
Juan de Nova Island
Mauritius
Bassas da India
Madagascar
Ile Europa
Reunion
Southern Kuriles
North Korea
Japan
Japan - Korea
Japan - South Korea Conflict Zone
South Korea
China
Conflict Zone
Taiwan
Paracel Islands
Vietnam
Spratly Islands
Palau
Micronesia
Philippines
Malaysia
Brunei
Singapore
Marshall Islands
Howland Isl. and Baker Isl.
Nauru
Kiribati
Papua New Guinea
Indonesia
Solomon Islands
Tuvalu
Australia/Indonesia
Vanuatu
American Samoa
Wallis and Futuna
Australia - Papua New Guinea
Fiji
Samoa
East Timor
New Caledonia
Niue
Tonga
Australia - East Timor
Australia
New Zealand
Macquarie Island
source
clockwise
sink
Antarctica
Asia Pacific
Caribbean
East Africa
Mediterranean
Middle East
North America
Northern Europe
South America
South Asia
West Africa
West Pacific

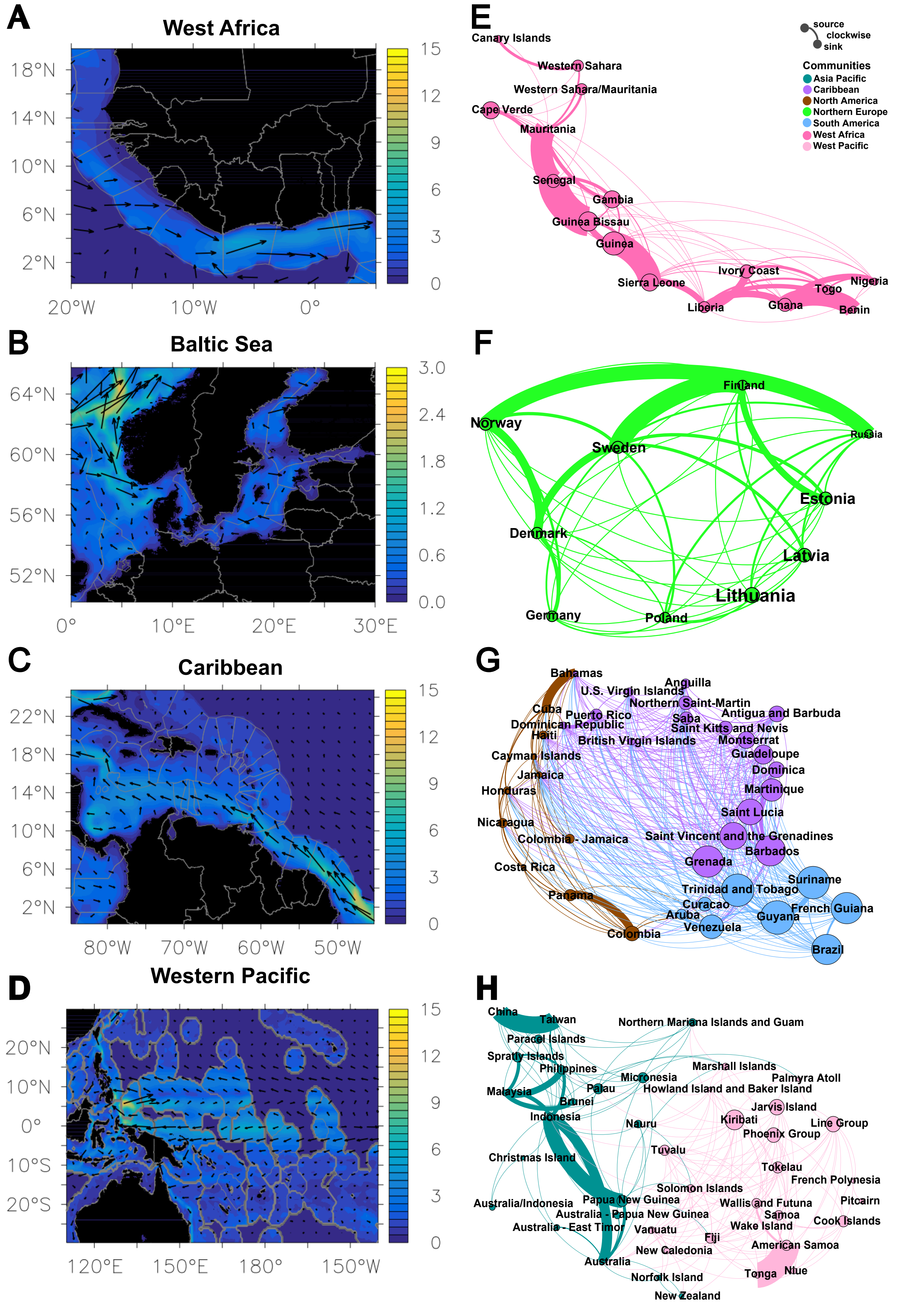

A
West Africa
18°N
14°N
10°N
6°N
2°N
20°W
10°W
0°
15
12
9
6
3
0
B
Baltic Sea
64°N
60°N
56°N
52°N
0°
10°E
20°E
30°E
3.0
2.4
1.8
1.2
0.6
0.0
C
Caribbean
22°N
18°N
14°N
10°N
6°N
2°N
80°W
70°W
60°W
50°W
D
Western Pacific
20°N
10°N
0°
10°S
20°S
120°E
150°E
180°
150°W
E
source
clockwise
sink
Communities
Asia Pacific
Caribbean
North America
Northern Europe
South America
West Africa
West Pacific
Canary Islands
Western Sahara
Western Sahara/Mauritania
Cape Verde
Mauritania
Senegal
Gambia
Guinea Bissau
Guinea
Sierra Leone
Ivory Coast
Liberia
Ghana
Togo
Nigeria
Benin
F
Finland
Norway
Russia
Sweden
Estonia
Denmark
Latvia
Lithuania
Germany
Poland
G
Bahamas
Anguilla
U.S. Virgin Islands
Northern Saint-Martin
Cuba
Puerto Rico
Antigua and Barbuda
Dominican Republic
Saba
Saint Kitts and Nevis
Haiti
British Virgin Islands
Montserrat
Cayman Islands
Guadeloupe
Dominica
Jamaica
Honduras
Martinique
Saint Lucia
Nicaragua
Saint Vincent and the Grenadines
Colombia - Jamaica
Barbados
Costa Rica
Grenada
Suriname
Trinidad and Tobago
Panama
Curacao
French Guiana
Aruba
Guyana
Venezuela
Colombia
Brazil
H
China
Taiwan
Northern Mariana Islands and Guam
Paracel Islands
Spratly Islands
Marshall Islands
Philippines
Palmyra Atoll
Micronesia
Malaysia
Palau
Howland Island and Baker Island
Brunei
Jarvis Island
Indonesia
Kiribati
Line Group
Nauru
Phoenix Group
Tuvalu
Christmas Island
Tokelau
French Polynesia
Solomon Islands
Australia/Indonesia
Papua New Guinea
Wallis and Futuna
Pitcairn
Australia - Papua New Guinea
Samoa
Cook Islands
Australia - East Timor
Vanuatu
Wake Island
Fiji
New Caledonia
American Samoa
Australia
Norfolk Island
Tonga
Niue
New Zealand

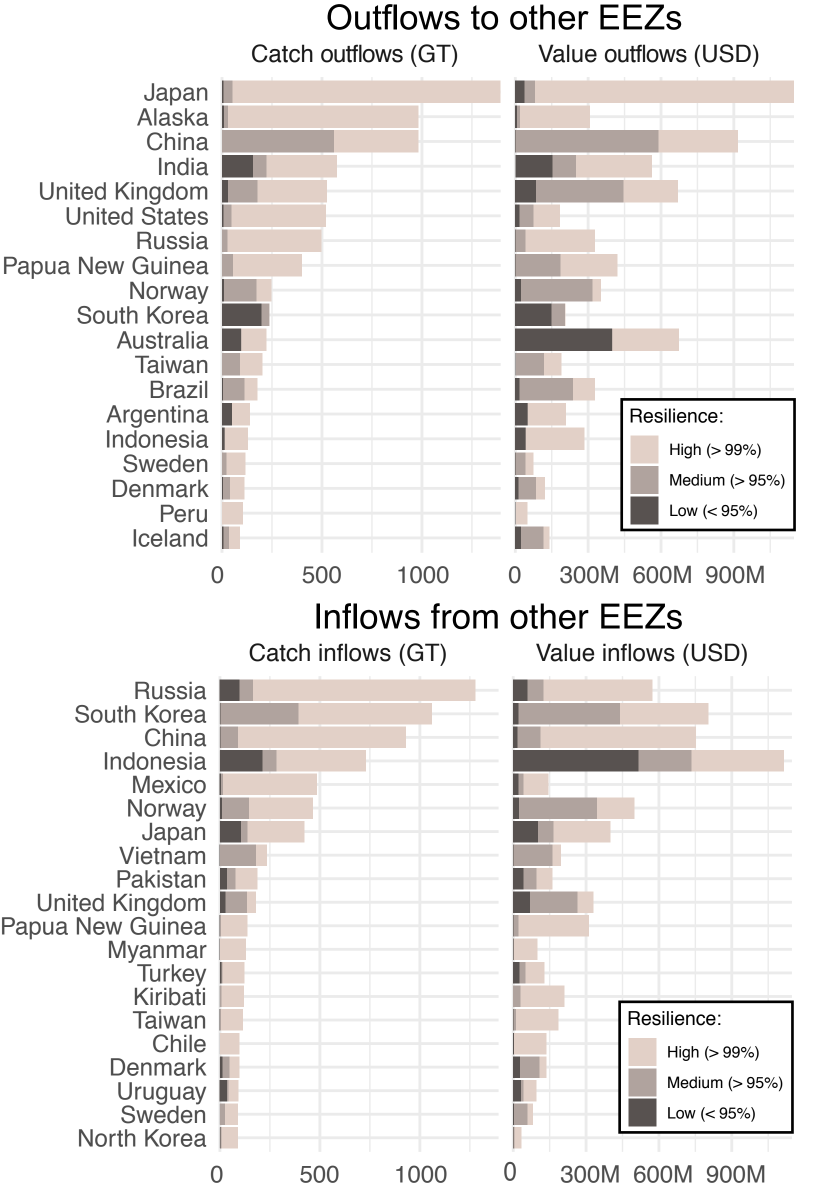

Outflows to other EEZs
Catch outflows (GT)
Value outflows (USD)
Japan
Alaska
China
India
United Kingdom
United States
Russia
Papua New Guinea
Norway
South Korea
Australia
Taiwan
Brazil
Argentina
Indonesia
Sweden
Denmark
Peru
Iceland
0
500
1000
0
300M
600M
900M
Resilience:
High (> 99%)
Medium (> 95%)
Low (< 95%)
Inflows from other EEZs
Catch inflows (GT)
Value inflows (USD)
Russia
South Korea
China
Indonesia
Mexico
Norway
Japan
Vietnam
Pakistan
United Kingdom
Papua New Guinea
Myanmar
Turkey
Kiribati
Taiwan
Chile
Denmark
Uruguay
Sweden
North Korea
0
500
1000
0
300M
600M
900M
Resilience:
High (> 99%)
Medium (> 95%)
Low (< 95%)

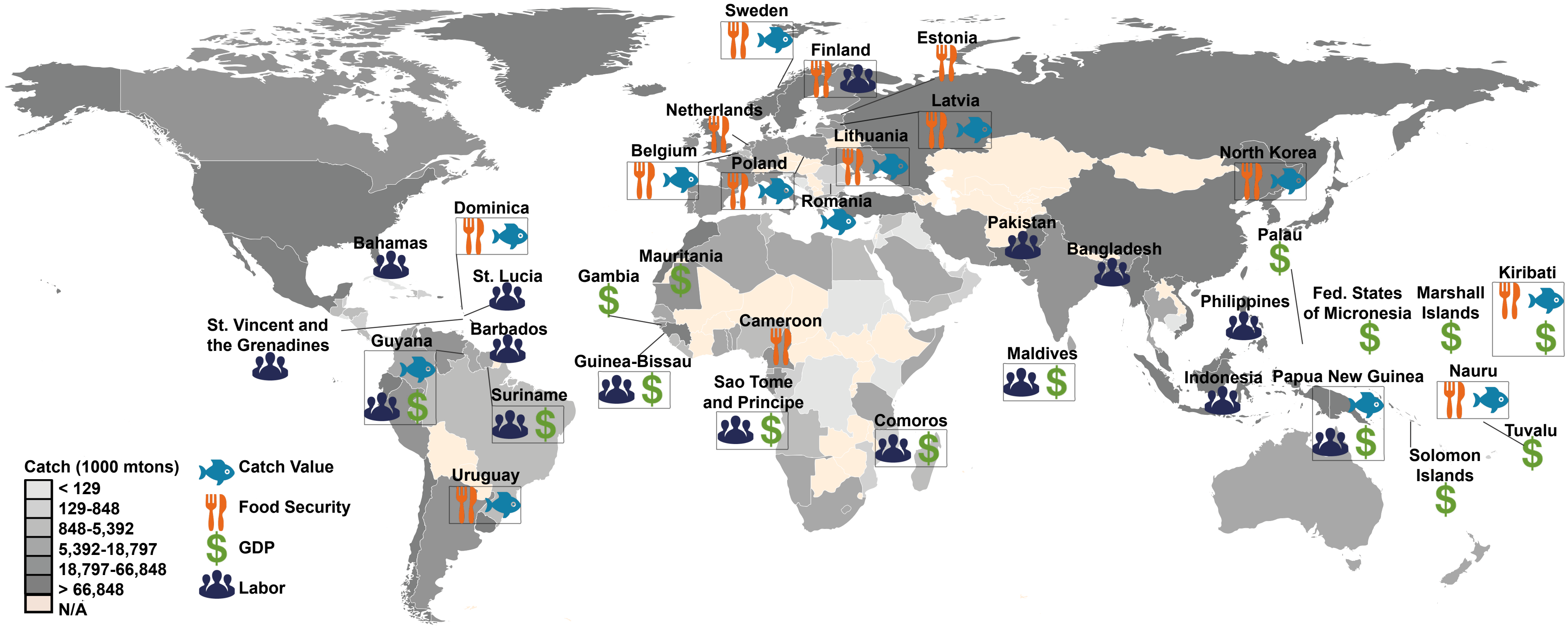
Sweden
Finland
Estonia
Latvia
Netherlands
Lithuania
Belgium
Poland
Romania
North Korea
Dominica
Bahamas
Pakistan
Palau
Bangladesh
Mauritania
Gambia
St. Lucia
Kiribati
Fed. States of Micronesia
Marshall Islands
Philippines
St. Vincent and the Grenadines
Barbados
Cameroon
Guyana
Guinea-Bissau
Maldives
Sao Tome and Principe
Suriname
Indonesia
Papua New Guinea
Nauru
Comoros
Tuvalu
Solomon Islands
Uruguay
Catch (1000 mtons)
< 129
129-848
848-5,392
5,392-18,797
18,797-66,848
> 66,848
N/A
Catch Value
Food Security
GDP
Labor

Figure Legends

Fig. 1 The network of spawn-attributed catch flows between EEZs. Each EEZ is a node (circle) of the network and its color represents its network community. The connectors or edges in this network flow clockwise from source to sink, with their thicknesses representing the magnitude of the net flow of caught biomass between the EEZs. Only the edges in the upper tercile of edge weights are shown here for clarity (see SM 3.2 for the full network). The size of each node represents its out-degree, i.e., the number of other EEZs for which it acts as a source of fish larvae, including connections not shown in this image.

Fig. 2 Regional currents and community networks Panels A-D display the speed (colors, cm/s) and direction (arrows) of ocean surface currents in four regions with interconnected fisheries (West Africa, Baltic Sea, the Caribbean, and Western Pacific) during the month of maximum spawning activity in each (August, May, June, and May respectively). Panels E-H display the corresponding subset of the global network encompassed by these regions. Colors, node sizing, and connector directions are as in Fig. 1. Nodes are arranged to approximately correspond to geographic locations of the EEZs.

Fig. 3 Countries with highest outflowing and inflowing catch. Top: Top 20 countries sorted by total outflowing catch (MT) and value (USD) at risk. **Bottom:** Top 20 countries sorted by total inflow of catch (MT) and value (USD) at risk. 2005 – 2014 values of catch and landed values are used, attributing them to larvae by species. Resilience levels represent the estimated decline a population can endure without being considered vulnerable to local extinction.

Fig. 4 Hotspot map showing fishing dependency on spawning grounds in neighboring waters by country. Countries are shaded by catch (mtons) at risk, with darker shades representing more catch. Icons depict EEZs that are the most dependent on their neighbors. The catch icon indicates that more than 30% of a country's catch value is dependent on neighboring spawning grounds, the GDP icon represents a risk to more than 0.8% of its GDP, the labor icon represents that more than 1.5% of its jobs are vulnerable, and the food security icon represents a value of greater than 1.1% of the food security dependence index.

Supplementary Materials

www.sciencemag.org/content/

Materials and Methods

Figs. S1-S14

Tables S1-S8

References (32-44)

SM 1 Method Summary

Spawn dispersal was estimated with the Connectivity Modeling System, a Lagrangian system (*22*), applied to ocean surface velocities (*23*) from a 20-year climatological average spanning the period from 1991 to 2010. At each location where spawning occurs, we release 100 simulated particles to obtain probabilistic estimates of the effects of turbulence. Particle EEZ-to-EEZ transitions were then organized into transition probability matrices, U_{mf}, for spawning in month m and a floating duration of f months, where row i, column j describes the portion of particles produced in EEZ i reaching EEZ j. We match fishery data from Sea Around Us (*18*) for 706 species and 434 genera across 280 regions with spawning region, month, and spawn characteristics from FishBase (*24, 31*), excluding anadromous species. The presence of spawning for species k in EEZ i during month m, s_{ikm}, and the spawn floating durations, f_k, are described in SM 2.2 and SM 2.3. We calculate the portion of species k that drifts from EEZ i to EEZ j as

$$(D_k)_{ij} = \begin{cases} \frac{p_{ik}}{\sum_i p_{ik}} \frac{\sum_m s_{ikm} (U_{m,f_k})_{ij}}{\sum_m s_{ikm}} & \text{if } \sum_m s_{ikm} > 0 \\ 0 & \text{otherwise} \end{cases}$$

where p_{ik} is the estimated suitability of species k in EEZ i if it spawns in EEZ i and 0 otherwise (see further derivation nodes in SM 3.3).

The distribution of the number of outward-directed spawn flows per EEZ (the out-degree distribution) is a key parameter for classifying the spawning network. The distribution of node out-degrees in the global fisheries network follows a power law (exponent of 1.55 ± 0.1), with a large number of nodes having small out-degrees, along with a "fat tail" consisting of nodes with high out-degrees (see Fig. S7). The network edge weights are $(W)_{ij} = \sum_k (D_k)_{ij}\text{Catch}_{kj}$, where Catch_{kj} is the average landed catch for species k in EEZ j from 2005 to 2014 from Sea Around Us (*18*).

The portion of species k in EEZ j attributed to external spawning is then $r_{kj} = 1 - \frac{(D_k)_{jj}}{\sum_i (D_k)_{ij}}$.

Total biomass imported to EEZ j is $\sum_k r_{kj}\text{Catch}_{kj}$ and the landed value imported is $\sum_k r_{kj}\text{LandedValue}_{kj}$. Landed values are similarly averaged from 2005 to 2014. The fraction of the EEZ j's fishery considered at risk is:

$$\frac{\sum_k r_{kj}\text{LandedValue}_{kj}}{\sum_k \text{LandedValue}_{kj}}$$

the fraction of GDP at risk is:

$$\frac{\sum_k r_{kj}\text{LandedValue}_{kj}}{\text{GDP}_j}$$

the fraction of jobs at risk is:

$$\frac{\sum_k r_{kj}\text{LandedValue}_{kj}}{\text{GDP}_j} \frac{\text{FisheryJobs}_j}{\text{LaborForce}_j}$$

and the index of food security dependency is:

$$\frac{\left((\text{Production}_j - \text{Export}_j)^{\sum_k r_{kj} p_k \text{Catch}_{kj} / \sum_k p_k \text{Catch}_{kj}} + \text{Import}_j\right) \text{ProteinFromFish}_j \text{ProteinRequirement}}{\left(\text{Production}_j - \text{Export}_j + \text{Import}_j\right) \text{ProteinFromAny}_j^2}$$

where ProteinFromFish is the amount of protein obtained from fish per capita, ProteinRequirement is the amount of protein required by adults, and ProteinFromAny is the total protein from all sources consumed per capita. (see SM 3.4 for interpretation).

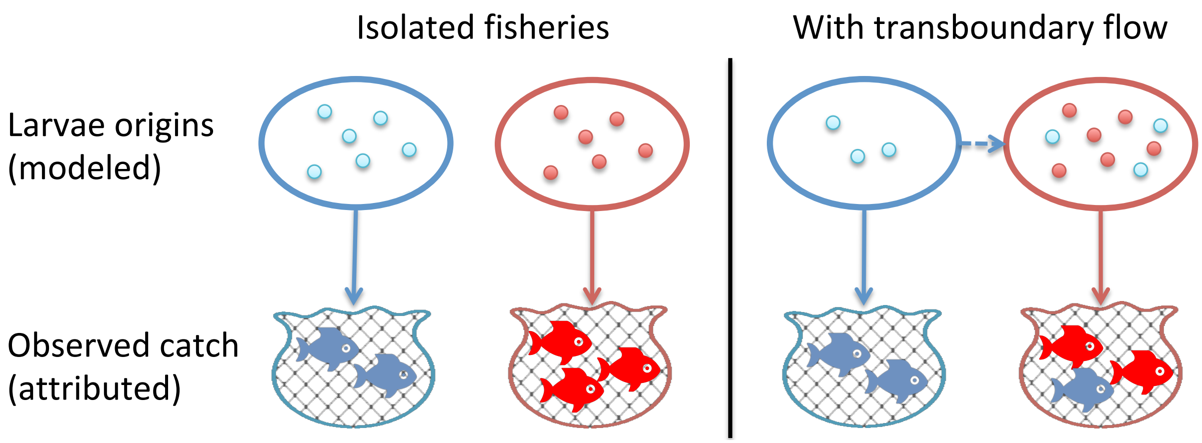

Fig. S1 A simple example to show the intuition behind our method. Dots represent modeled flow particles, which represent the dispersal of larvae prior to settlement. On the left, two isolated fisheries are shown, and all observed catch is attributed to spawn produced within each fishery. After modeling transboundary flow, on the right, the right fishery has a mix of larvae from local and foreign origins. The portion of catch attributable to each fishery equal the portion of particles, assuming that local and foreign larvae are subject to the same mortality and settlement success rates and have the same catchability.

SM 1.1 Intuition relating spawn to catch

Our analysis made the simplifying assumption that catch is proportional to the final location of spawn, as modeled by particles subject to ocean currents. The intuition behind this assumption is shown in Fig. S1.

After a period of floating, we assumed that spawn that originated within national boundaries are indistinguishable from those that originated elsewhere. Although most spawn will not survive to adulthood, we assumed that foreign and local spawn are subject to the same mortality rates. Since those that survive are furthermore indistinguishable to fishers and equally subject to fishing effort, the portion of caught fish attributable to each originating country match the portion of particles that arrive from each country.

The average EEZ receives cross-boundary spawn from 86 different species, across 54 genera.

Throughout the paper, we focused on the consequences of these spawn floating dynamics for human appropriation. As a result, we study catch, rather than the underlying stock dynamics. However, it is important to note that these cross-boundary spawning effects play an important role in each region's ecology and biodiversity, and future work should study their implications for conservation.

SM 2 Data collection

A summary of the data collected and the coverage of data sources across species is shown in Table S1. Of the 1398 species and 996 genera included in the Sea Around Us dataset, we were able to match 706 species and representatives of 434 genera to spawning data, and this is the subset that we used for our analysis. Of the genera, 41 are only represented in Sea Around Us at the genus level (as unspecified species), resulting in a total of 747 distinct taxonomic groups.

SM 2.1 Fishery industry data

From Sea Around Us (*18*), we collected species fished and their yearly catch and landed value. Sea Around Us includes reconstructions of industrial, artisanal, subsistence, and recreational fisheries (*32*). While the data quality of Sea Around Us is very heterogeneous across countries, it is the most widely used global data set on fish catch. Data is provided at the Exclusive Economic Zone (EEZ) level, and this formed the spatial unit of our analysis throughout.

Sea Around Us identified the species or genus for 84.4% of global catch and 85.5% of global landed value. The remaining catch was lumped together, and cannot be modeled here. The fish included in our analysis represent 51% of total marine catch (about 60 billion USD) and 38%

Split by data available:	SAU	Spawning	AquaMaps	Larvae Level	# Species	# Genuses
	✓	✓	✓	species	236	0
	✓	✓	✓	genus	101	73
	✓	✓	✓	family	109	145
	✓	✓	✓	order	50	82
	✓	✓	✓	class	54	71
	✓	✓	✓	phylum	1	4
	✓	✓		species	76	0
	✓	✓		genus	18	7
	✓	✓		family	24	19
	✓	✓		order	15	17
	✓	✓		class	22	16
Included Species	706	706	551	1780	706	
Included Genera	434	434	375	18		434

Table S1 Data collection summary. The first 11 rows count the number of species and genera for which each of the given collections of data is available. The last two rows sum the total number of species for which data is available for each dataset. The Larvae Level column lists the level at which larval floating durations are determined for each species or genus included in that row. The totals for the Larvae Level column include both data drawn from Fishbase for SAU species and additional records provided as an online supplement.

of total marine landed value (about 55 million mtons).

SM 2.2 Spawning information

To estimate the total distance traveled during the dispersal period, we collected data on the location and month of fish spawning and the duration of the larval stage for each species. We retrieved the species summary information, larvae dynamics, egg development, and spawning regions and months from the FishBase database (*24*). From the summary information for each species, we identified anadromous species and exclude these from the dataset. We combined spawning data listed if FishBase with spawning countries and months from the Science and Conservation of Fish Aggregations (SCRFA) database (*31*).

Within-country localities were matched to sub-country EEZs where available, and spawning regions spanning multiple countries were matched to all included EEZs. Some FishBase entries provide relative spawning abundance across months, between 0 and 100%. s_{ikm} is defined for the given EEZ i, species k, and month m as the maximum relative abundance across matching spawning entries, treating SCRFA spawning records and un-weighted FishBase records as a relative abundance of 100%.

In our spawning data, 244 unique countries are observed (all coastal countries except Azerbaijan and Turkmenistan on the Caspian Sea). The maps in Figure S2 highlight the EEZs of countries which are identified as having spawning activity in each month, for the 2098 species and 499 genera for which we have spawning location data, identified from all available species and genera represented in Sea Around Us. This species count is greater than the species count in the data table above, because we collect all available species-specific spawning data for genera that are not identified at the species level in Sea Around Us.

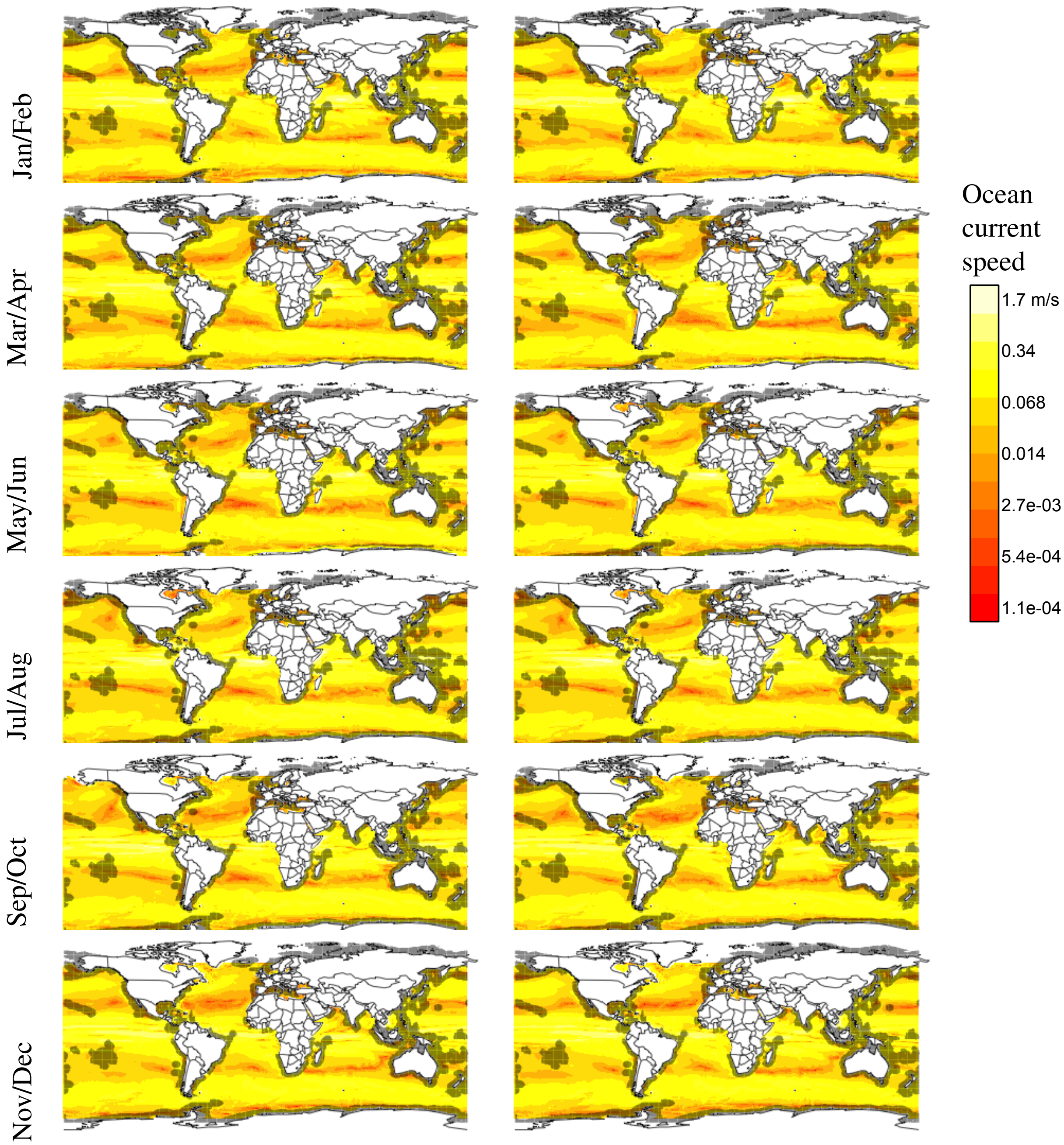

Fig. S2 Ocean current speed maps and areas of active spawning in each month of the year. Darkened masks show areas of active spawning in each month of the year. Colors represent monthly average ocean current velocities, on a log scale.

SM 2.3 Spawn floating characteristics

Most marine fish species float for a period during their early development, as floating eggs and planktonic larva (*33*). The FishBase database contains the duration and characteristics of this period for 361 species and 9 genera from our species list (*24*). Durations for species in some top economically important fish groups with floating data in FishBase are shown in table SM 2.6 and figure S3. Table SM 2.6 also shows the intermediate information used to determine these durations.

Species	Larval Duration	Egg Duration	Egg Floating	Float Bounds
Clupea harengus	160	NA	fixed	160
Decapterus pinnulatus	NA	0.38	buoyant	≥ 0.38
Decapterus polyaspis	NA	1.50	buoyant	≥ 1.5
Engraulis japonicus	47	1.50	buoyant	48.5
Engraulis ringens	74	NA	buoyant	> 74
Gadus morhua	100	25.00	buoyant	125
Katsuwonus pelamis	20	1.10	buoyant	21.1
Micromesistius poutassou	0	7.75	buoyant	7.75
Nemipterus virgatus	NA	1.00	buoyant	≥ 1
Rastrelliger kanagurta	NA	NA	buoyant	> 0
Sardina pilchardus	40	NA	buoyant	> 40
Sardinella neohowii	NA	1.00	buoyant	≥ 1
Scomber japonicus	17	2.06	buoyant	19.06
Scomber scombrus	40	6.00	buoyant	46
Scomberomorus cavalla	12	NA	unknown	≥ 12
Scomberomorus maculatus	9	1.00	unknown	9 - 10
Sprattus sprattus	NA	6.25	buoyant	≥ 6.25
Theragra chalcogramma	108	NA	buoyant	> 108
Thunnus albacares	25	1.40	buoyant	26.4
Trachurus symmetricus	0	1.5	buoyant	1.5
Trichiurus lepturus	NA	6.00	buoyant	≥ 6

Table S2 Available information in the FishBase database on larvae dynamics and fish egg development for some top commercial species. The Float Bounds column represents a summary of the other columns and is not a true representation of the bounds of possible range of floating durations since the other columns only give approximate means.

The estimated duration for which species k is subject to floating along surface currents, f_k, is

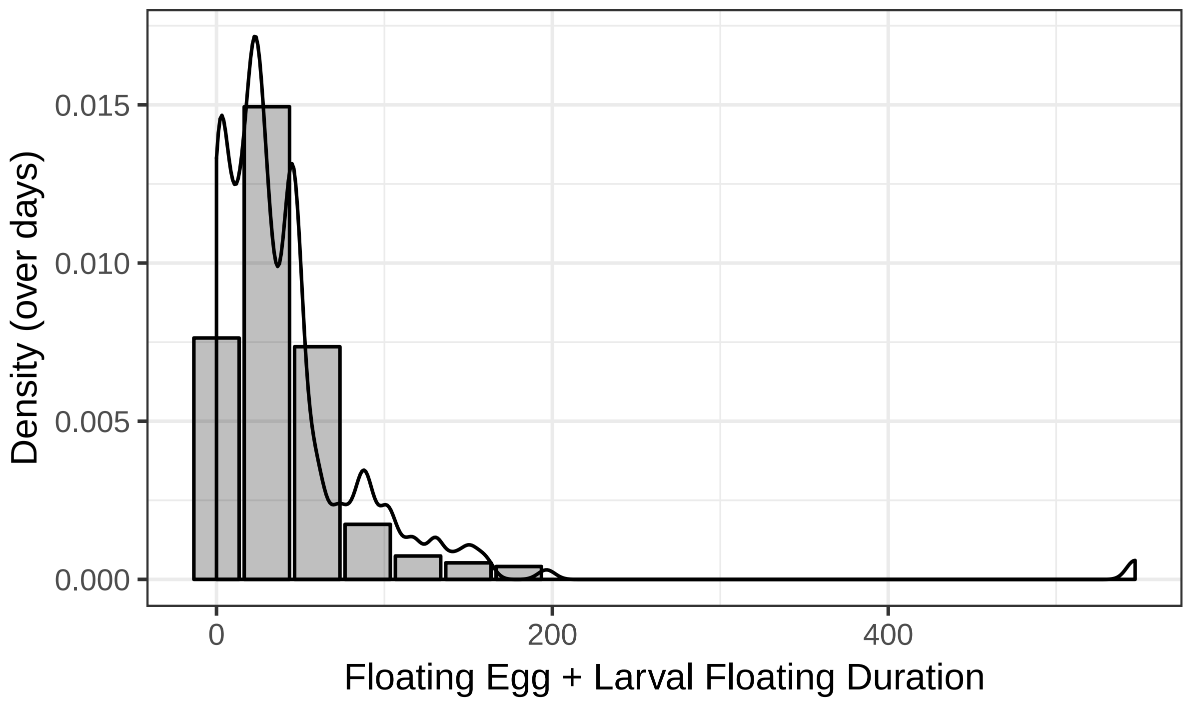

Fig. S3 Distribution of total floating time for recorded species, overlaid with the histogram of applied durations across all species. The floating time is the larvae duration, plus egg duration in the cases where the egg is floating and the data is available. Species without observed larval characteristics use a Monte Carlo of durations from the lowest-taxonomic level at which data is observed. The line shows the distribution for recorded species. The histogram is at the monthly level, with durations as actually used in the analysis.

the duration of the larval stage, plus the duration of its egg stage if the eggs are buoyant. If the eggs are buoyant but the egg stage duration is not provided, a floading egg period of 4 days is used, the average buoyant egg stage. These durations are then rounded to the nearest month in the analysis. If information on the larval duration was not available for species k, then a Monte Carlo across all durations available for the genus was used. Similarly, if no data is available at the genus-level, we used the family, order, class, or phylum of the species, stopping at the lowest level at which data is available.

SM 2.4 Species prevalence

The AquaMaps database describes estimated population distribution maps, which are further subject to expert review (*34*). The maps are based on observed relationships between species occurrence and environmental factors including bottom depth, temperatures, salinity, primary production, sea ice concentration, and distance to land. Prevalence data for each species is represented as a 0.5° by 0.5° grid, with values from 0 to 1. We calculate the sum of grid-level species prevalence by EEZ to produce p_{ik}. These data are used to scale spawning activity amongst observed spawning countries.

SM 2.5 Ocean Velocity Data

We used the Simple Ocean Data Assimilation (SODA) version 2.2.4 (Carton and Giese 2008), a widely-used product that assimilates available ocean observations from satellites as well as in-situ measurements and makes use of an ocean model to fill in gaps in the data to produce a complete dataset of monthly mean velocities on a 3-dimensional regular grid. The resolution of the dataset is 0.5° x 0.5° in the horizontal. Ocean velocities are resolved into three-dimensional vectors oriented zonally (i.e., parallel to latitude), meridionally (parallel to longitude), and vertically (parallel to the radius of the Earth at each point) for each grid cell. We made use of monthly mean zonal and meridional velocities in the uppermost layer (from the sea surface to a depth of 10 m) of the grid, and neglected vertical velocities as they are small (typically 10^{-7} ms^{-1} at their largest) compared to horizontal velocities (which are typically between 0.01 and 0.1 ms^{-1}) and unlikely to affect the trajectories of fish spawn.

For our simulation, we made use of data from the years 1991 to 2010 to calculate climatological averages, i.e., an "average year" by computing the average zonal and meridional vectors at each spatial point for each calendar month over the 20-year period. This averaging removed the biases in ocean surface currents that can arise when a single year alone is used due to climate events such as El Nino and La Nina, which can cause large changes in current velocities within a single year, while preserving the month-to-month changes in ocean current speeds and directions that are characteristic of the annual cycle.

SM 2.6 Average spawning month speeds

Fig. displays the distribution of current speeds across spawning regions and months for the top species in Table , to given an indication the potentially considerable speeds to which these spawn are subject. The median velocity is $0.092\,\mathrm{m/s}$ (95% CI 0.088 - 0.102).

The average current speed in spawning regions was computed by the following steps.

For each of the species, the spawning data specifies which months spawning has been reported within specified regions. We associated these regions with country EEZs.

Of the species for which we have spawning data, 551 also have population distribution maps available in AquaMaps (*34*). Within each of these EEZs, let the population distribution of fish for a given species be $D_i(x, y) = D(x, y) \cap EEZ_i$. Let the corresponding current speed across space in month m be $S_m(x,y)$. The average spawn speed is calculated as $\frac{\iint_{x,y} D_i(x,y) S_m(x,y)}{\iint_{x,y} D_i(x,y)}$.

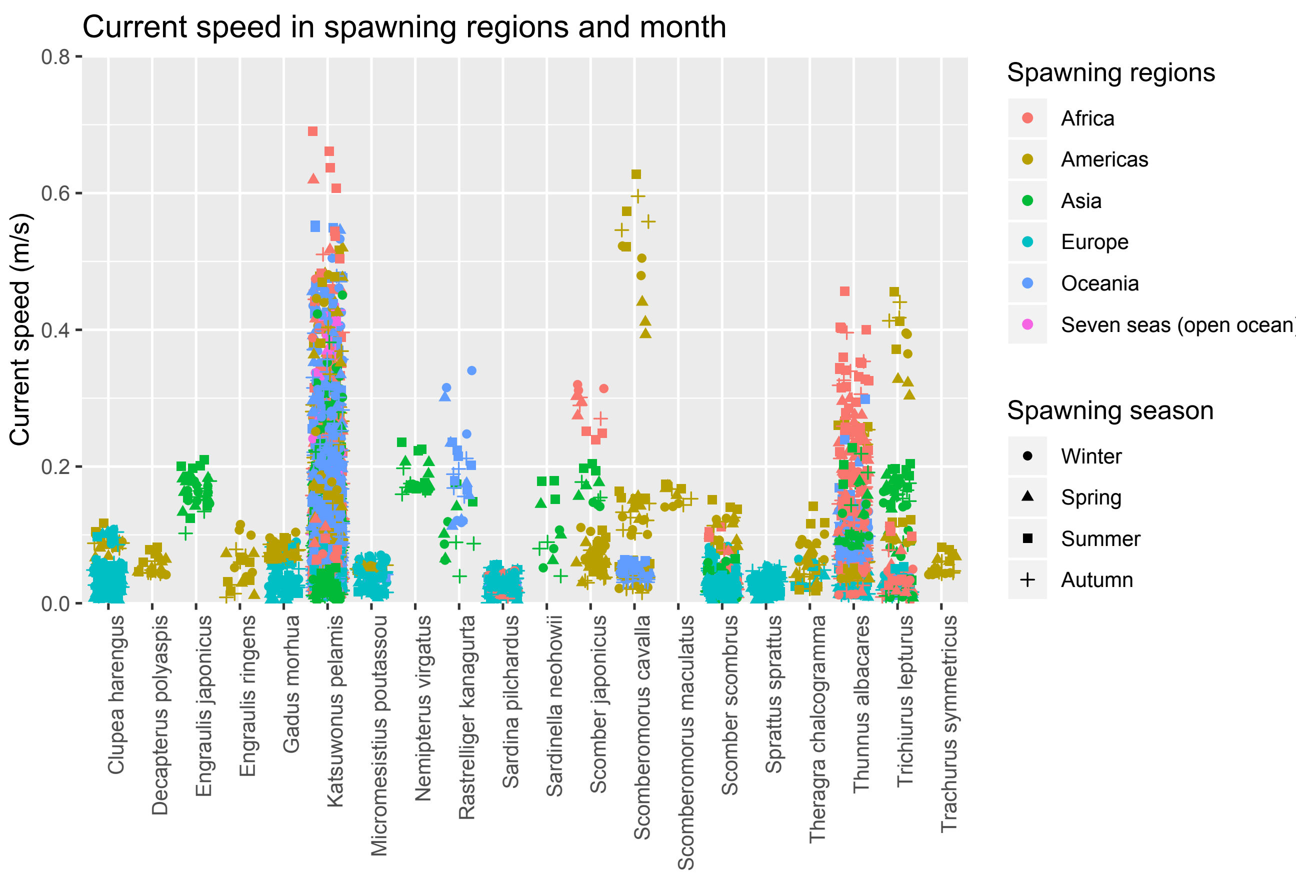

Fig. S4 Current speeds in spawning regions and months. Ocean current speeds in spawning regions and months for some top commercial species. Each point represents a region-month where the given species (displayed along the horizontal axis) is spawning.

SM 3 Analysis

SM 3.1 Estimation of connectivity

SM 3.1.1 Lagrangian Scheme

The estimates of larval connectivity between EEZs were made using the Connectivity Modeling System (CMS) (Paris et al 2013) Lagrangian scheme. The CMS is a software package which, given a time-evolving ocean velocity field resolved into 2- or 3-dimensional vectors and a set of initial particle positions, computes the trajectories of those particles through the ocean.

The CMS performs a spatiotemporal interpolation in order to estimate the velocity, and thereby the position, of each particle in the simulation at each time step based on the input velocities. In order to simulate the effects of subgrid-scale stochastic motions, a random walk scheme is used to provide an additional velocity in a random direction to the particles. The additional velocity is scaled according to a diffusivity coefficient of 1000 m^2/s. This value is appropriate for this resolution over large areas of the Earth's surface, although the horizontal diffusivity coefficient can take significantly higher values in a few limited regions (*35*). While this scheme cannot provide an exact reconstruction of the particle trajectories that occurred, it can be used instead to obtain a probabilistic estimate of the effect of these motions by using multiple particles beginning at a single initial position.

SM 3.1.2 Simulations

We provided the CMS with zonal and meridional components of velocity at every grid point of the surface layer of the SODA dataset in order to arrive at our estimates of larval dispersal. The particles representing larval flows were introduced in the calendar months and locations where spawning is known to occur based on the data from sources described above, and allowed to disperse for six months from initialization. As ocean surface currents undergo large variations between seasons, including complete reversals in direction over the course of each year in monsoon regions, initializing the particles during the specific months of spawning for each species is crucial to obtaining the correct direction of larval flows. In order to estimate a distribution over the effects of the random-walk turbulence scheme, 100 particles were placed at each of the starting locations. The final location of each particle was ascertained as the location of the particle at the end of the drifting duration based on the larval drifting duration data available for its species. For floating durations greater than 6 months, a duration of 6 months was used.

We do not assign a constant amount of biomass per particle in our simulation and instead performed the following procedure to estimate the flow of biomass. In each destination or “sink” EEZ, and for each species, we assessed the proportion of larvae that arrived from each of the origin or “source” EEZs, summed over all months. The amount of catch represented by the incoming particles from each source EEZ is then estimated as the corresponding proportion of the observed catch for the given species in that EEZ. Instead of assuming a mortality rate for the larvae, regarding which data is scarce, the particles that drift to regions where its species is not known to be caught were assumed not to have survived their journey. We exclude Diadromous fish.

This procedure was repeated for each species found in each EEZ and summed over all species in order to arrive at an estimate of the net flow of catch between each pair of EEZs. These flows then formed the connections seen in the network shown in the main text.

SM 3.1.3 Resolution

The ocean currents dataset is at a 0.5° x 0.5° resolution, which does not allow features of the currents close to shore to be resolved. Figure S5 (a) shows the distribution of value attributable to cross-boundary flow from our analysis, distributed according to the 90th percentile depth of the species. According to this metric, only 1.2% of this value is attributable to species that are confined to this zone close to shore.

(a) Cross-boundary value by distance from shore (b) Distribution of species by depth

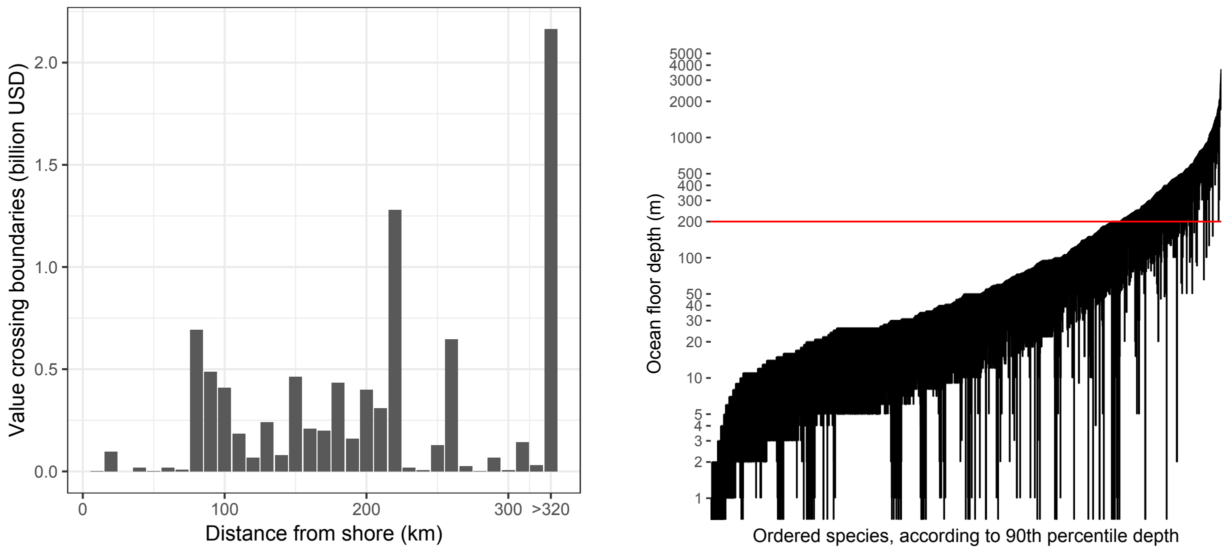

Fig. S5 Distributions of species based on distance from shore and depth. (A) shows the distribution of value of cross-boundary flow based on the distance from shore where species are found. (B) shows the distribution of species ordered by the 90th percentile of the depths at which they are found. The red line indicates 200 m, the depth which we use to define the continental shelf.

We do distinguish between species that spawn and settle along the continental shelf and those that do so further out. In this case, we considered the ocean depths at which the species is found. About 20% of species have a 90th percentile depth beyond $200\,\mathrm{m}$ (see figure S5 (b)). For these species, we allowed spawning and settling of particles across the whole EEZ; for the remaining species, we only used the portion of the EEZ on the continental shelf, defined as having an ocean depth less than $200\,\mathrm{m}$.

SM 3.2 Network Analysis

SM 3.2.1 Summary of Network Properties

Table S3 summarizes the properties of the global network of marine fisheries arising from larval dispersal. The network displays the small-world property, as seen by the weighted and unweighted small-coefficients, which are both greater than one. The network's mean path length, that is, the average shortest distance between all pairs of nodes in the network measured as the number of nodes crossed, is 5.14. This shows that the network, despite having 226 nodes, can be traversed in a small number of steps and highlights the highly-interconnected nature of the network of marine fisheries. Figure S6 shows the full network. Note that edges in this system can be as small as 10^{-12}, meaning that the probability of larval dispersal along the thinnest edges shown in the figure are highly unlikely.

Network Property	Value
Number of Nodes	226
Number of Edges	2059
Mean Path Length	5.14
Clustering Coefficient	0.69
Weighted Clustering Coefficient	0.71
Small-Coefficient	2.99
Weighted Small-Coefficient	914
Average Out-Degree	8.83
Average In-Degree	8.72

Table S3 A summary of the properties of the global network of marine fisheries.

SM 3.2.2 Determination of Scale-Free Property

The defining characteristic of scale-free networks is that their degree distributions follow a power law. For directed networks, the out-degree and in-degree distributions are considered separately as they may represent different phenomena. We consider the out-degree distribu-

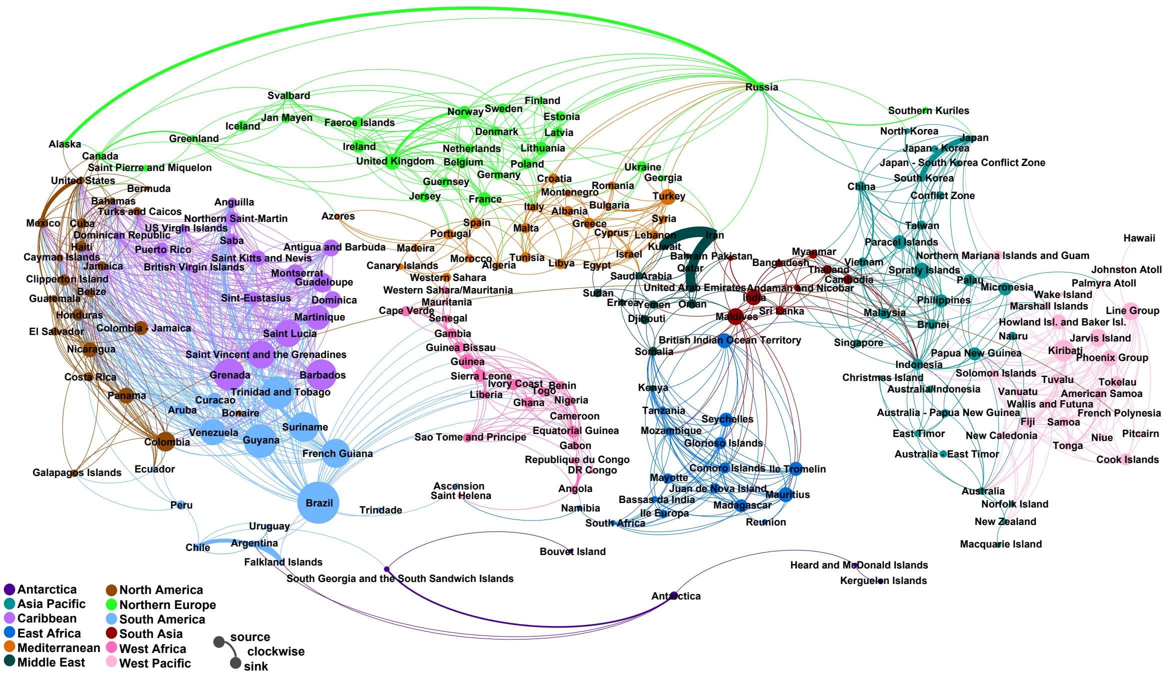

Fig. S6 The full network of cross-boundary flows of catch based on larval dispersal. Node sizes reflect the number of outward connectors, i.e., out-degree, of the node. The colors represent the communities. Connectors flow clockwise from source to sink.

tion in this study, as this represents the propagation of fish eggs and larvae outwards from the EEZ of spawning, and also contains information on the propagation of disturbances in the network.

We fit a power-law to the weighted out-degree distribution in order to test whether this network is scale-free. As the shape of the curve can vary depending on the number of bins used to estimate the distribution, we performed the fit for every possible number of bins from 30 to 50. The exponent is found to remain stable within the range of bins tested, with a mean value of 1.54 and standard deviation of 0.002. The p-values for the power-law fit within this range have a mean of 0.007 and standard deviation of 0.0015. The fit of a power-law curve for a distribution with 40 bins is shown in Figure S7.

SM 3.2.3 Determination of Small-World Property

The network is found to be a small world network by calculating its weighted small-coefficient, i.e., the ratio of the weighted clustering coefficient to the mean shortest path, relative to a random network of the same size (*36, 37*). Networks that have a small-coefficient greater than one are considered to have the small-world property. For the global network of fisheries, we found the value of the small-coefficient to be 914.

The small-coefficient is given by the following formula:

$$\frac{C}{L} \Big/ \frac{C_R}{L_R}$$

where L is the mean shortest path length in the network, C is the clustering coefficient of the network, L_R is the mean shortest path length in a random network of the same size as the network of interest, and C_R is the clustering coefficient of a random network of the same size as the network of interest. In a weighted network such as that being considered, the weighted clustering coefficient (*38*) and weighted mean path length were used (*37*) as C and L respectively.

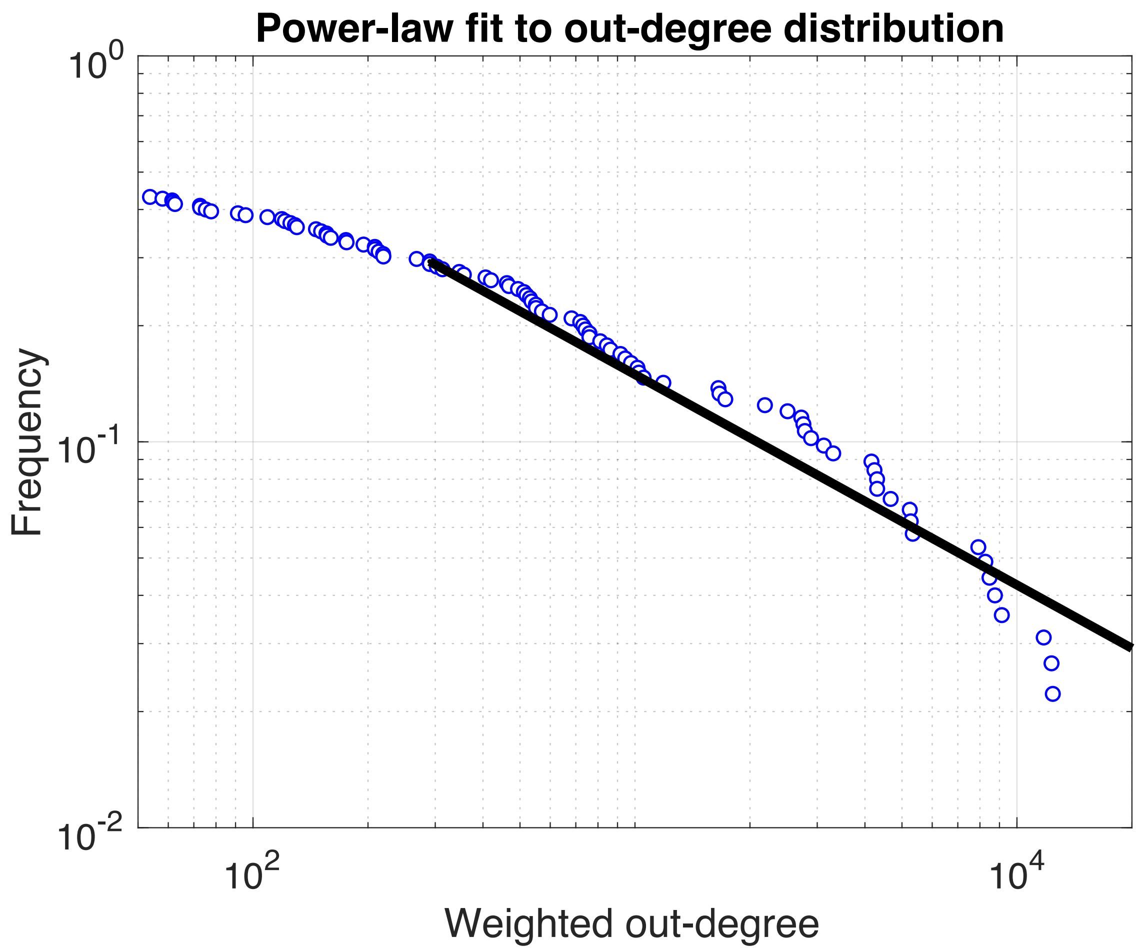

Fig. S7 A log-log plot of the weighted out-degree distribution of the network. The distribution of weighted out-degrees of the network's nodes is shown by blue dots and the fitted power-law curve is shown as a black line.

To compute L_R and C_R for comparable random networks, we generated 100 networks by randomly permuting the edges of the global network as in Bolanos et al., 2013. We then took the average mean shortest path length and clustering coefficients, respectively, over these 100 networks.

SM 3.2.4 Properties of Communities

We detected the communities within the global network using the Louvain community-detection algorithm for undirected graphs (*39*). This results in twelve communities that correspond approximately to geographic regions. For the individual communities within the global network, we computed the small-coefficient using the same procedure as above. Table S4 displays the properties of the complete network followed by those of each of the communities found within the network, listed in descending order of their small-coefficients. Only three of these communities – South America, East Africa, and Northern Europe – do not exhibit the small-world property (since the Antarctic community is too small to determine a weighted clustering coefficient, we do not calculate its small-coefficient). The small-coefficients are highest for the Caribbean and West Pacific communities, where large hubs such as Barbados and Kiribati are visible in the network.

SM 3.3 Species-level risk

To determine socioeconomic risk, we first translated the physical transition matrix of particle transitions, U_{mf}, defined for each month m and floating duration f, into a spawning transition matrix, T_k. T_k is the transition matrix of the spawn of species k, and is the weighted average of the physical transition matrix over its spawning months. We used spawning observations (see appendix SM 2.2) to construct s_{ikm}, which is 1 if species k spawns in EEZ i in month m. For

Community	Nodes	Edges	Weighted Clustering Coefficient	Mean Shortest Path Length	Weighted Small-coefficient
Global	226	2059	0.71	5.41	914
Caribbean	18	214	0.998	1.55	4281000
West Pacific	25	142	0.714	2.15	124659
South Asia	9	45	0.829	1.40	22440
North America	21	170	0.774	1.69	18581
West Africa	22	162	0.785	2.01	3215
Mediterranean	24	160	0.773	2.24	938
Middle East	13	53	0.775	1.77	547
Asia Pacific	29	153	0.755	2.1	152
Northern Europe	28	221	0.762	1.86	0.181
East Africa	16	95	0.844	1.86	0.062
South America	16	57	0.737	2.6	0.003

Table S4 The small-world properties of the entire network and each of the communities within it.

each species k, we calculated the spawn transition matrix

$$
\begin{aligned}
(T_k)_{ij} &= \frac{\sum_m s_{ikm} (U_{m,f_k})_{ij}}{\sum_m s_{ikm}} && \text{if } \textstyle\sum_m s_{ikm} > 0 \\
&= 0 && \text{otherwise}
\end{aligned}
$$

where $(\cdot)_{ij}$ is the element of that matrix at row i (representing the EEZ at the initial position) and column j (representing the EEZ at the final position), and f_k is the floating duration for species k. In the case where species k uses a Monte Carlo over different duration estimates, $(T_k)_{ij}$ is an average of the matrices computed for each value of f_k.

Next, we generated a version of the transition matrix, D_k, which is weighted by the portion of spawning that occurs in each EEZ in which species k spawns. The spawning records do not provide a relative estimate of the amount of spawning occurring in each region, so we took the product of spawning regions with species suitability to estimate relative spawning abundance. We assumed that species spawn in proportion to their suitability across those EEZs in which they spawn. Let p_{ik} be the suitability of species k in EEZ i, from AquaMaps (*34*), if $s_{ikm} > 0$ for any month m, and 0 otherwise. Then, the relative spawning distribution for species k across EEZs i is

$$q_{ik} = \frac{p_{ik}}{\sum_i p_{ik}}$$

We defined the portion of species k that drifts from EEZ i to EEZ j:

$$(D_k)_{ij} = q_{ik}(T_k)_{ij}$$

Note that $\sum_{ij}(D_k)_{ij} = 1 \, \forall k$.

Although the calculations above are at the species level, with biological presence and spawning characteristics available for individual species, catch records are often only available for commercial groups. We defined E_g, the portion of commercial group g that drifts from EEZ i to EEZ j, as the average across its component species:

$$(E_g)_{ij} = \frac{\sum_{k \in K(g)}(D_k)_{ij}}{|K(g)|}$$

where $K(g)$ is the set of species contained in commercial group g and $|K(g)|$ is the number of species in group g.

The portion of the recruitment arriving in EEZ j that originated in EEZ i is a ratio of $(E_g)_{ij}$ to all EEZs indexed by l.

$$(F_g)_{ij} = \frac{(E_g)_{ij}}{\sum_l (E_g)_{il}}$$

The portion of commercial group g caught in EEZ j that originated in other countries, and therefore may be at risk in the absence of international cooperation, is $r_{jg} = 1 - (F_g)_{jj}$.

To determine the socioeconomic impacts and risks of these spawning transitions, we applied each commercial group's portion of spawning originating in other countries to its total landed value and total catch. These values are collected from Sea Around Us (*18*) and averaged over 2005 to 2014. The catch at risk in EEZ i is then $\text{EEZCatchRisk}_i = \sum_k r_{ig}\text{Catch}_{ig}$, where Catch_{ig} is the total catch (in mtons) of commercial group g in EEZ i. Similarly, $\text{EEZLandedValueRisk}_i = \sum_k r_{ig}\text{LandedValue}_{ig}$.

Table S5 displays the results of this analysis for each EEZ region. Figure S8 displays the value and catch imported from other EEZs, ordered from most to least. Between the 9th and the 170th EEZs with the most imported catch and value from spawn, these quantities closely follow an exponential decay in rank, where each country has approximately $(4.55 \pm 0.02)\,\%$ less value and $(5.11 \pm 0.03)\,\%$ less catch attributable to other countries than the country before it.

EEZ	Sovereign	Avg. te3	Avg. $M	Risk te3	Risk $M
China	China	9852.0	17293.7	928.4	751.6
Peru	Peru	8582.6	3781.2	63.2	42.0
Indonesia	Indonesia	7576.9	10621.7	729.2	1115.2
Russia	Russian Federation	7199.8	4659.7	1276.8	572.9
Japan	Japan	4809.8	10102.9	421.4	400.9
India	India	4047.7	4962.8	16.0	25.9
Chile	Chile	3458.2	2908.5	97.5	137.3
United States	United States	3392.5	11317.0	50.5	53.8
South Korea	Korea, Dem. Rep.	3353.8	4862.0	1060.9	802.3
Vietnam	Vietnam	3274.5	3459.1	234.4	196.8
Malaysia	Malaysia	3228.7	4677.3	81.5	152.8
Morocco	Morocco	2909.0	4391.0	67.3	131.1
Alaska	United States	2446.3	1769.4	52.8	54.5
Norway	Norway	2287.6	3242.7	465.6	498.2
Mexico	Mexico	2138.2	3030.3	484.2	145.1
Mauritania	Mauritania	2088.4	2857.7	49.2	67.5
Philippines	Philippines	2076.7	2468.8	85.1	163.8
Thailand	Thailand	1875.8	2766.8	14.4	29.8
Myanmar	Myanmar	1780.4	2242.7	129.3	100.0
United Kingdom	United Kingdom	1631.1	3276.6	180.5	331.1
Argentina	Argentina	1338.0	1510.0	46.1	79.4
Iceland	Iceland	1162.0	1728.6	80.0	87.2
Canada	Canada	1106.7	3151.0	65.8	85.1
Bangladesh	Bangladesh	982.6	802.9	46.3	46.1
Cambodia	Cambodia	893.5	919.8	0.0	0.0
Brazil	Brazil	869.7	1937.4	2.8	5.5

EEZ	Sovereign	Avg. te3	Avg. $M	Risk te3	Risk $M
Guinea	Guinea	857.9	1482.1	86.0	25.8
Pakistan	Pakistan	839.5	853.4	188.0	160.5
Senegal	Senegal	777.7	1315.2	12.9	35.6
Turkey	Turkey	740.2	1154.8	120.8	128.8
New Zealand	New Zealand	707.1	1402.3	9.3	22.4
Angola	Angola	686.0	1473.2	1.8	3.7
South Africa	South Africa	678.6	643.3	5.9	1.6
Ireland	Ireland	590.4	1118.2	53.4	61.7
Namibia	Namibia	570.9	600.2	8.7	9.8
Sri Lanka	Sri Lanka	542.1	598.9	7.2	9.3
Guinea Bissau	Guinea-Bissau	538.3	845.4	19.4	44.9
Faeroe Islands	Denmark	519.0	935.5	80.6	123.0
Spain	Spain	514.3	1610.4	34.6	113.1
Nigeria	Nigeria	508.9	1082.0	2.2	5.4
Papua New Guinea	Papua New Guinea	434.5	858.4	138.7	312.6
Ghana	Ghana	431.0	498.6	13.6	15.1
Falkland Islands	United Kingdom	419.1	1184.7	27.4	44.0
Yemen	Yemen, Rep.	416.5	464.6	1.2	2.4
France	France	392.9	1271.6	47.3	164.7
Italy	Italy	373.1	2063.3	54.4	385.5
Iran	Iran, Islamic Rep.	368.1	581.4	48.1	88.4
Taiwan	China	348.6	531.1	114.3	186.1
Ecuador	Ecuador	346.6	347.4	81.7	40.1
Sierra Leone	Sierra Leone	296.0	221.4	2.2	3.3
Sweden	Sweden	288.0	224.0	91.1	80.3
Greenland	Denmark	277.1	795.6	32.2	76.1
Denmark	Denmark	265.7	482.4	96.9	136.5
Algeria	Algeria	250.0	549.3	12.6	29.9
North Korea	Korea, Rep.	245.5	204.5	88.9	33.8
Venezuela	Venezuela, RB	236.0	555.7	28.1	79.2
Portugal	Portugal	227.1	478.2	18.4	63.2
Australia	Australia	222.8	1126.0	8.6	39.0
Oman	Oman	209.4	441.2	0.1	0.4
Gambia	Gambia, The	203.4	233.6	4.3	6.0
Gabon	Gabon	196.2	250.5	32.2	24.6
Micronesia	Micronesia, Fed. Sts.	188.8	391.7	33.6	86.8
Germany	Germany	188.4	502.2	45.9	69.1
Kiribati	Kiribati	184.6	357.0	119.9	210.3
Greece	Greece	184.3	964.6	12.8	121.4
Svalbard	Norway	177.9	340.0	71.9	100.3
Solomon Islands	Solomon Islands	170.5	375.9	10.7	19.5
Ivory Coast	Côte d'Ivoire	167.3	200.9	2.2	4.1
Egypt	Egypt, Arab Rep.	162.7	233.7	4.6	12.3

EEZ	Sovereign	Avg. te3	Avg. $M	Risk te3	Risk $M
Georgia	Georgia	160.7	96.6	17.7	12.4
Somalia	Somalia	154.2	268.4	7.0	4.6
Madagascar	Madagascar	152.3	273.6	1.0	1.8
Cameroon	Cameroon	145.2	151.4	56.2	21.3
Mozambique	Mozambique	145.1	209.9	0.2	0.8
Panama	Panama	143.2	208.4	0.1	0.1
Netherlands	Netherlands	133.7	351.2	56.1	97.4
Uruguay	Uruguay	132.7	159.1	91.8	95.7
Poland	Poland	132.1	114.0	60.5	71.5
Tanzania	Tanzania	115.4	203.7	6.1	3.5
Tunisia	Tunisia	111.9	199.3	5.3	15.5
Finland	Finland	109.5	61.1	49.5	17.0
Liberia	Liberia	105.6	156.3	1.6	2.4
Ukraine	Ukraine	102.2	66.5	29.8	13.0
Libya	Libya	101.9	225.3	11.0	57.1
Maldives	Maldives	98.6	191.5	18.2	39.7
Latvia	Latvia	96.1	44.5	32.1	16.7
Saudi Arabia	Saudi Arabia	95.1	317.6	5.6	17.1
République du Congo	Congo, Rep.	89.2	128.0	0.4	1.0
Andaman & Nicobar	India	85.3	78.0	9.3	11.0
Galapagos Islands	Ecuador	85.1	119.1	3.6	5.2
Croatia	Croatia	77.8	92.9	6.8	9.2
United Arab Emirates	United Arab Emirates	75.9	260.1	0.2	0.6
Estonia	Estonia	75.3	30.3	24.3	8.4
Benin	Benin	75.2	88.6	14.7	6.3
Palau	Palau	70.8	158.0	17.4	43.1
Guyana	Guyana	68.0	87.9	12.3	27.3
Phoenix Group	Kiribati	67.3	125.2	37.0	65.1
Suriname	Suriname	66.5	98.8	13.4	26.4
Colombia	Colombia	66.3	99.6	18.5	7.0
Canary Islands	Spain	65.9	205.5	18.9	59.2
Nauru	Nauru	65.4	139.7	52.2	98.8
Togo	Togo	63.9	83.0	8.6	11.2
Costa Rica	Costa Rica	62.2	96.5	3.3	7.0
Bahrain	Bahrain	54.6	205.9	2.2	6.6
Dominican Republic	Dominican Republic	50.8	103.1	0.5	1.0
SGSSI	United Kingdom	43.7	83.2	1.4	4.1
Fiji	Fiji	43.0	149.2	0.4	1.2
Tuvalu	Tuvalu	41.5	77.9	5.4	10.1
Hawaii	United States	41.3	202.4	0.0	0.0
Marshall Islands	Marshall Islands	41.1	89.7	4.1	8.6
Guatemala	Guatemala	41.0	56.8	2.5	5.1
Kuwait	Kuwait	39.6	65.6	0.0	0.0

EEZ	Sovereign	Avg. te3	Avg. $M	Risk te3	Risk $M
Equatorial Guinea	Equatorial Guinea	38.4	87.4	1.8	4.4
Nicaragua	Nicaragua	37.8	83.9	0.3	0.6
Jamaica	Jamaica	34.5	59.8	0.1	0.4
El Salvador	El Salvador	34.3	35.3	0.0	0.0
Cuba	Cuba	30.3	68.6	0.1	0.3
French Polynesia	French Polynesia	28.0	103.1	0.1	0.2
Congo, Dem. Rep.	Congo, Dem. Rep.	25.3	43.9	0.1	0.1
Haiti	Haiti	25.2	42.9	1.6	3.1
Line Group	Kiribati	24.2	67.3	0.5	2.0
Cape Verde	Cabo Verde	23.5	58.5	0.0	0.1
Lithuania	Lithuania	22.7	13.8	9.3	8.2
Trinidad & Tobago	Trinidad & Tobago	21.1	49.3	0.6	1.2
Brunei	Brunei Darussalam	21.1	31.6	0.4	0.5
Bahamas	Bahamas, The	20.6	125.1	3.7	9.3
Vanuatu	Vanuatu	19.1	30.5	0.3	0.5
Comoro Islands	Comoros	18.9	29.3	4.7	7.0
Bulgaria	Bulgaria	18.5	21.0	0.5	3.0
Azores	Portugal	18.5	47.7	0.6	1.3
Mauritius	Mauritius	18.2	50.8	0.0	0.1
Qatar	Qatar	18.1	80.5	0.1	0.3
French Guiana	France	18.0	44.9	2.5	6.9
Honduras	Honduras	17.1	48.6	1.0	1.5
Samoa	Samoa	16.2	30.7	0.5	0.7
Kenya	Kenya	15.9	40.3	0.1	0.1
Sao Tome & Principe	Sao Tome & Principe	15.1	33.5	1.5	3.4
New Caledonia	France	13.8	52.4	0.1	0.2
Turks & Caicos Islands	United Kingdom	11.2	31.8	0.1	0.3
Cook Islands	New Zealand	11.1	22.6	0.0	0.0
Seychelles	Seychelles	11.0	16.8	0.1	0.1
Guadeloupe	France	11.0	24.4	0.6	3.0
Eritrea	Eritrea	10.3	12.7	0.0	0.0
Tokelau	New Zealand	9.8	19.3	0.0	0.1
Bassas da India	France	9.2	13.6	2.4	3.5
Madeira	Portugal	7.9	20.2	0.9	2.1
American Samoa	American Samoa	7.9	20.1	0.1	0.2
Lebanon	Lebanon	7.9	15.4	0.6	1.2
Clipperton Island	France	7.5	13.4	0.0	0.0
Martinique	France	7.3	20.5	0.3	1.3
Tonga	Tonga	7.1	12.2	0.1	0.2
Belgium	Belgium	7.1	27.8	3.5	12.4
Jan Mayen	Norway	7.1	12.1	0.2	0.5
British Indian Ocean Territory	United Kingdom	7.0	7.4	0.0	0.2
Belize	Belize	6.9	11.3	0.3	0.7

EEZ	Sovereign	Avg. te3	Avg. $M	Risk te3	Risk $M
Iraq	Iraq	6.7	19.1	0.0	0.0
Syria	Syrian Arab Republic	6.2	12.9	1.0	2.1
East Timor	Timor-Leste	6.2	10.9	0.3	0.3
Kerguelen Islands	France	5.9	47.0	0.0	0.0
Trindade	Brazil	5.5	11.1	0.0	0.0
Singapore	Singapore	5.5	6.9	0.1	0.3
Barbados	Barbados	4.9	5.6	0.2	0.4
Albania	Albania	4.6	6.9	0.2	1.3
Cyprus	Cyprus	4.2	15.1	0.6	3.3
Antigua & Barbuda	Antigua & Barbuda	3.9	12.5	0.0	0.0
British Virgin Islands	United Kingdom	3.8	19.2	0.3	2.0
Malta	Malta	3.6	13.1	0.9	3.5
Howland Island & Baker Island	United States	3.6	11.8	0.0	0.0
St. Pierre & Miquelon	France	3.5	9.2	0.9	2.5
Djibouti	Djibouti	3.4	7.3	0.0	0.0
Heard & McDonald Islands	Australia	3.3	26.1	0.6	2.4
Réunion	France	2.9	9.8	0.0	0.0
St. Vincent	St. Vincent	2.9	8.9	1.0	2.1
Sudan	Sudan	2.9	6.6	0.0	0.0
Grenada	Grenada	2.7	5.0	0.6	0.9
Mayotte	France	2.7	12.1	0.4	1.4
Ile Tromelin	France	2.4	3.6	0.1	0.2
Aruba	Netherlands	2.3	6.1	0.4	1.1
St. Lucia	St. Lucia	2.2	3.9	0.5	1.0
Puerto Rico	United States	2.0	5.5	0.0	0.0
Romania	Romania	1.8	4.7	0.5	1.8
St. Kitts & Nevis	St. Kitts & Nevis	1.6	6.9	0.1	0.5
Anguilla	United Kingdom	1.6	10.3	0.0	0.0
Dominica	Dominica	1.6	4.4	0.7	1.7
Wallis & Futuna	France	1.5	5.9	0.1	0.4
Curaçao	Netherlands	1.4	5.4	0.0	0.1
Johnston Atoll	United States	1.4	2.1	0.0	0.0
Montenegro	Montenegro	1.4	2.8	0.2	0.8
US Virgin Islands	United States	1.3	4.5	0.1	0.2
Easter Island	Chile	1.2	3.1	0.0	0.0
Crozet Islands	France	1.0	7.1	0.0	0.0
Bermuda	United Kingdom	0.9	5.8	0.0	0.1
Northern Saint-Martin	France	0.9	4.6	0.1	0.5
Niue	New Zealand	0.8	1.5	0.0	0.0
Sint-Maarten	Netherlands	0.8	1.8	0.0	0.0
Slovenia	Slovenia	0.8	2.0	0.0	0.0
Bonaire	Netherlands	0.7	2.0	0.0	0.0
Amsterdam & St. Paul Islands	France	0.6	1.7	0.0	0.0

EEZ	Sovereign	Avg. te3	Avg. $M	Risk te3	Risk $M
Northern Mariana & Guam	United States	0.5	1.9	0.0	0.0
Jarvis Island	United States	0.5	2.1	0.0	0.0
Tristan da Cunha	United Kingdom	0.5	7.9	0.0	0.0
Prince Edward Islands	South Africa	0.4	2.5	0.0	0.0
St. Helena	United Kingdom	0.4	1.3	0.0	0.0
Saba	Netherlands	0.4	3.0	0.0	0.0
Sint-Eustasius	Netherlands	0.4	3.0	0.0	0.0
Jordan	Jordan	0.3	0.5	0.0	0.0
Macquarie Island	Australia	0.3	2.2	0.0	0.0
Cocos Islands	Australia	0.2	1.1	0.0	0.0
Cayman Islands	United Kingdom	0.2	0.4	0.1	0.2
Glorioso Islands	France	0.2	0.3	0.0	0.0
Ascension	United Kingdom	0.1	0.2	0.0	0.0
Norfolk Island	Australia	0.1	0.2	0.0	0.0
Bouvet Island	Norway	0.1	0.1	0.0	0.0
Palmyra Atoll	United States	0.1	0.4	0.0	0.2
Bosnia & Herzegovina	Bosnia & Herzegovina	0.1	0.1	0.0	0.0
Montserrat	United Kingdom	0.1	0.2	0.0	0.0
Christmas Island	Australia	0.1	0.2	0.0	0.1
Pitcairn	United Kingdom	0.0	0.1	0.0	0.0
Wake Island	United States	0.0	0.0	0.0	0.0

Table S5 Summary of the inflows of tonnage and landed value by region. For each country, the *Avg. te3* column reports the landed catch (in 1000 mtons), and the *Avg. $M* column reports the landed value (in millions of 2010 USD), averaged over 2005 - 2014. Of this total, a portion is attributable to inflows of spawn from other EEZs. These values are reported in the *Risk te3* and *Risk $M* columns (labeled as "at risk" since management outside of national control can undermine them). For each region, we also list the sovereign country, at which results are aggregated for the hotspot risk measures.

SM 3.4 Country-level risk

Comprehensive risk measures are calculated at the sovereign country level, where GDP, fishery employment, and food scarcity measures are available. Let c index sovereign countries, and $I(c)$ be the set of EEZs in country c. While $I(c)$ includes only 1 EEZ for most countries, it includes more in cases like the United States and France.

The catch at risk in country c is then $\text{CatchRisk}_c = \sum_{i \in I(c)} \text{EEZCatchRisk}_i$, and $\text{LandedValueRisk}_c =$

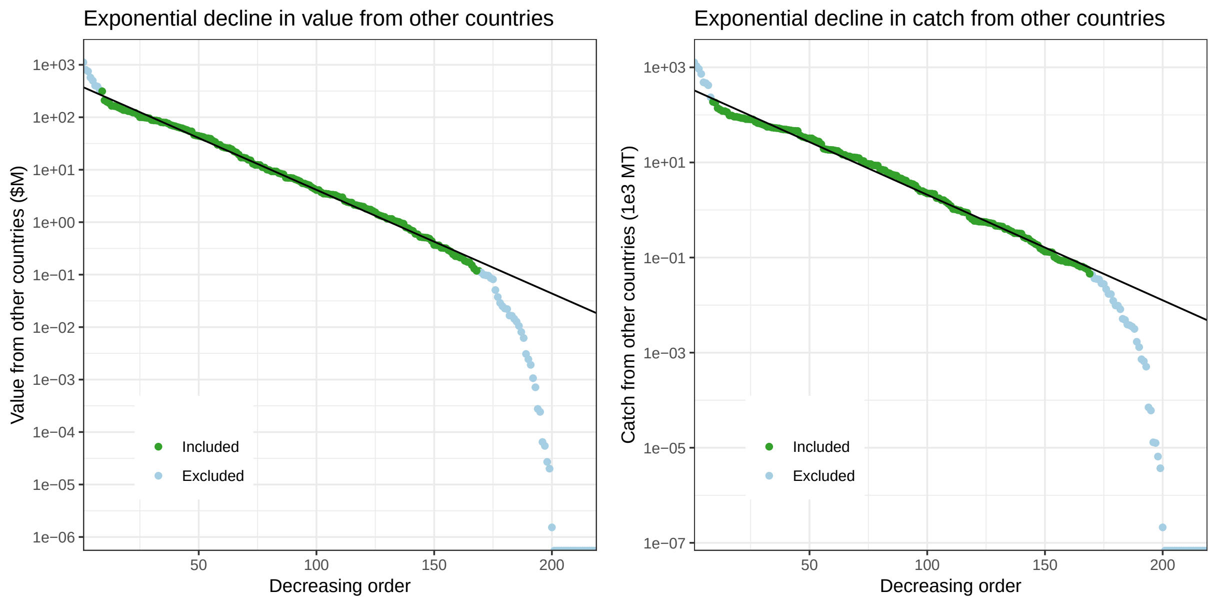

Fig. S8 The landed value (Left) and catch (Right) attributable to spawn from other countries, for each EEZ, ordered from the one with the most imported to the least. These follow an exponential decline for the majority of the range (labeled "included").

$\sum_{i \in I(c)} \text{EEZLandedValue}_i$. The countries with the most total catch and total fishery value at risk are generally those with the largest fisheries in total with 4 of the top 6 countries with the most catch at risk falling into the largest 5 fisheries globally by catch.

The fraction of a fishery's value at risk is ${}^{\text{LandedValueRisk}_c}\!/\!{}_{\sum_{i \in I(c)} \sum_k \text{LandedValue}_{ig}}$.

The fraction of country c's GDP at risk is ${}^{\text{LandedValueRisk}_c}\!/\!{}_{\text{GDP}_c}$, where GDP_c is the average GDP over 2005 to 2014.

The fraction of country c's jobs at risk is $\left({}^{\text{LandedValueRisk}_c}\!/\!{}_{\sum_{i \in I(c)} \sum_k \text{LandedValue}_{ig}}\right) \left({}^{\text{FisheryJobs}_c}\!/\!{}_{\text{LaborForce}_c}\right)$, where FisheryJobs_c is from Teh and Sumaila (*40*) and the labor force statistics are from the World Bank, derived with data from the International Labour Organization, and averaged over 2005 to 2014.

The risk to the country c's food security is calculated as

$$\frac{\left((\text{Production}_c - \text{Export}_c)\left(\sum_{i\in I(c)}\sum_k r_{ki}p_k\text{Catch}_{ki}\right)/\left(\sum_{i\in I(c)}\sum_k p_k\text{Catch}_{ki}\right) + \text{Import}_c\right)\text{ProteinFromFish}_c\text{ProteinRequire}}{(\text{Production}_c - \text{Export}_c + \text{Import}_c)\,\text{ProteinFromAny}_c^2}$$

This is derived as the product of the following terms:

$$\frac{\left((\text{Production}_c - \text{Export}_c)\left(\sum_{i\in I(c)}\sum_k r_{ki}p_k\text{Catch}_{ki}\right)/\left(\sum_{i\in I(c)}\sum_k p_k\text{Catch}_{ki}\right) + \text{Import}_c\right)}{(\text{Production}_c - \text{Export}_c + \text{Import}_c)}$$

which represents the fraction of the locally-consumed, locally-produced catch that is attributable to spawn originating in other nations' waters, plus imported fish which is considered not at risk. The denominator of this term represents the baseline consumption of fish.

Above, p_k is a species-specific weighting factor based on protein composition, described below. The protein percentage of fish varies from less than 9% by mass to over 25% by mass. Since our quantification of food security risk depends on fish protein, not all fish should be weighted equally.

For each species, we translated the catch into protein mass, using percent protein by weight factors from (*41*). Their dataset contains 57 species, including 6 arthropods, 5 mollusks, and 18 orders of fish. To estimate the protein portion for species not in their dataset, we averaged across the lowest shared taxonomic level for which there is data.

$$\frac{\text{ProteinFromFish}_j/\text{ProteinFromAny}_j}{\text{ProteinFromAny}_j/\text{ProteinRequirement}}$$

This term is the food security dependency index as defined by Barange et al. (*28*). The numerator of this term represents the fraction of the country's protein consumption that is from fish, and the denominator represents the fraction of the daily recommended protein intake [i] that is

[i] The daily recommended protein intake is 60 kg (average world weight (*42*)) times 0.8g protein per kg (The Dietary Reference Intakes from `http://nationalacademies.org/hmd/Activities/Nutrition/SummaryDRIs/DRI-Tables.aspx`)

available to the country's population. Thus, this index takes a larger value for those nations where the daily nutritional requirements of its population are not being met, indicating an outsize dependence on fish as a crucial source of protein.

Table S6 shows the range of protein portions and the number of species from Sea Around Us matched at each taxonomic level. The interquartile range of protein shares across all observed species is 17.9% to 19.5% protein by mass.

	Taxonomic Level	Count	Protein (Range, %)
1	species	46	9.5 - 25.2
2	genus	110	10.3 - 25.2
3	family	236	9.5 - 23.2
4	order	1049	9.5 - 23.2
5	class	322	12.5 - 20.4
6	phylum	66	13.4 - 18.9
7	kingdom	49	17.8

Table S6 The range of protein portion, by mass, by the taxonomic level at which species are matched to protein data.

Table S7 displays the results of these analyses for each country and figure S9 displays the metrics for countries with the most at risk.

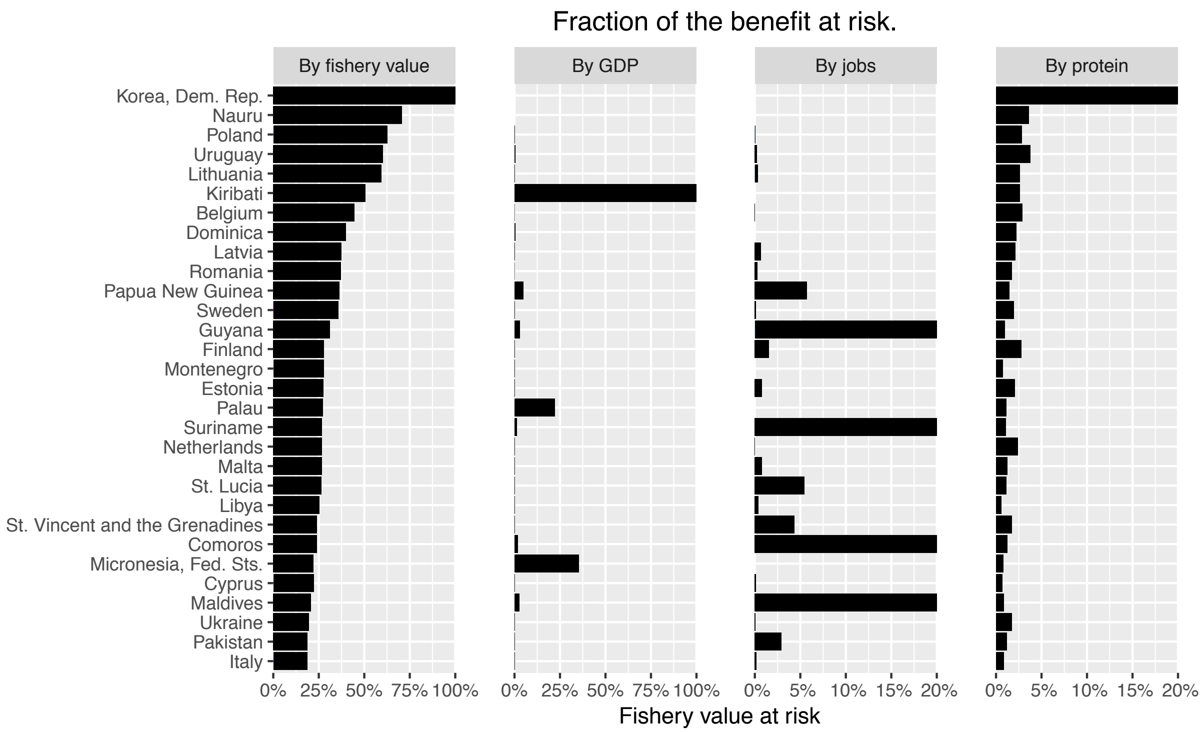

Fig. S9 Normalized values of well-being at risk, for the top 30 country's as ranked by the portion of their fishery sector at risk. *By fishery value* is the value at risk divided by the country's total landed value, averaged over the last 10 years. *By GDP* is the value at risk divided by the country's GDP, as a measure of the entire economy at risk. *By Jobs* takes the values in the *By fishery value* column and multiplies them by the portion of the population involved in direct and indirect fisheries work. *By protein* is an index of the risk in needed fishery protein for health.

Sovereign	Avg. MTe3	Avg. $M	GDP $M	Pop. (1e6s)	Workers (1e3s)	Protein P.C.	Fish Protein	R. value (%)	R. GDP (%)	R. jobs (%)	R. protein (%)
China	10200.6	17824.8	3531013.6	1330.9	730.0	236.6	48.6	5.3	0.0	0.0	0.6
Peru	8582.6	3781.2	99314.6	29.0	440.0	26.1	5.8	1.1	0.0	0.0	0.0
Indonesia	7576.9	10621.7	362691.5	237.3	25000.0	17.4	9.6	10.5	0.3	2.3	0.5
Russian Federation	7199.8	4659.7	903603.8	142.6	1200.0	54.1	7.5	12.3	0.1	0.2	1.0
United States	5889.5	13317.2	13680812.5	306.3	470.0	70.7	5.2	0.8	0.0	0.0	0.1
Japan	4809.8	10102.9	4653872.5	127.6	560.0	49.1	18.6	4.0	0.0	0.0	0.5
India	4132.9	5040.8	1147996.8	1190.0	94000.0	12.1	1.6	0.7	0.0	0.1	0.0
Chile	3459.4	2911.6	145739.5	17.0	130.0	44.4	4.4	4.7	0.1	0.1	0.2
Korea, Rep.	3353.8	4862.0	1055336.7	49.2	610.0	44.7	15.8	0.7	0.0	0.0	0.1
Vietnam	3274.5	3459.1	74438.2	86.0	12000.0	31.8	8.6	5.7	0.3	1.3	0.4
Malaysia	3228.7	4677.3	173832.7	27.8	430.0	43.1	16.8	3.3	0.1	0.1	0.1
Morocco	2909.0	4391.0	72573.6	31.4	620.0	24.3	4.1	3.0	0.2	0.2	0.1
Norway	2472.7	3594.9	318309.4	4.8	66.0	64.4	15.1	16.7	0.2	0.4	1.3
Mexico	2138.2	3030.3	954496.5	116.5	750.0	40.3	3.1	4.8	0.0	0.1	1.3
United Kingdom	2119.8	4629.2	2503059.4	62.3	38.0	58.4	5.4	8.3	0.0	0.0	0.6
Mauritania	2088.4	2857.7	2223.0	3.5	190.0	33.0	3.1	2.4	3.0	0.4	0.1
Philippines	2076.7	2468.8	126366.7	92.0	11000.0	24.9	9.7	6.6	0.1	1.9	0.2
Thailand	1875.8	2766.8	203093.8	66.3	4700.0	24.2	8.4	1.1	0.0	0.1	0.0
Myanmar	1780.4	2242.7		51.6	6900.0	34.1	14.5	4.5		1.3	0.4
Argentina	1338.0	1510.0	281004.9	40.0	54.0	64.6	1.8	5.3	0.0	0.0	0.2
Iceland	1162.0	1728.6	18350.4	0.3	16.0	96.2	28.0	5.0	0.5	0.4	0.4
Canada	1106.7	3151.0	1237121.9	33.7	130.0	57.8	5.8	2.7	0.0	0.0	0.3
Denmark	1061.7	2213.5	268521.6	5.5	38.0	68.3	9.2	15.2	0.1	0.2	1.2
Bangladesh	982.6	802.9	77663.6	149.7	16000.0	9.8	5.5	5.7	0.1	1.6	0.3
Cambodia	893.5	919.8	8451.7	14.2	960.0	17.8	11.3	0.0	0.0	0.0	0.0
Brazil	875.3	1948.6	1038220.1	193.4	2500.0	51.0	2.7	0.3	0.0	0.0	0.0
Guinea	857.9	1482.1	3248.2	10.6	640.0	8.7	2.8	1.7	0.8	0.3	0.6
Pakistan	839.5	853.4	127026.6	170.1	8800.0	26.5	0.6	18.8	0.1	2.9	1.2
Senegal	777.7	1315.2	9975.9	12.6	650.0	16.1	7.0	2.7	0.4	0.4	0.1
Turkey	740.2	1154.8	562487.3	71.3	610.0	32.8	2.2	11.2	0.0	0.3	1.0
New Zealand	728.9	1445.8	121169.1	4.3	24.0	65.8	7.0	1.6	0.0	0.0	0.1
Angola	686.0	1473.2	46325.8	19.0	430.0	17.3	4.3	0.3	0.0	0.0	0.0
South Africa	679.0	645.9	284535.5	50.3	110.0	34.3	1.7	0.3	0.0	0.0	0.1
Ireland	590.4	1118.2	218609.4	4.5	23.0	59.6	5.3	5.5	0.0	0.1	0.5
Spain	580.2	1815.9	1210030.6	45.8	200.0	65.2	12.9	9.5	0.0	0.1	0.5
Namibia	570.9	600.2	8827.7	2.2	24.0	23.9	3.9	1.6	0.1	0.0	0.1
Sri Lanka	542.1	598.9	31982.7	20.3	1600.0	16.3	9.2	1.6	0.0	0.3	0.1
Guinea-Bissau	538.3	845.4	669.1	1.6	660.0	8.8	0.3	5.3	6.7	5.5	0.2
Nigeria	508.9	1082.0	147985.5	155.9	4700.0	10.3	4.4	0.5	0.0	0.0	0.0
France	481.3	1542.1	2294746.5	64.7	110.0	71.0	9.4	12.0	0.0	0.0	0.6
Papua New Guinea	434.5	858.4	6297.9	6.7	490.0			36.4	5.0	5.7	1.4
Ecuador	431.8	466.5	48823.8	14.8	740.0	41.4	2.1	9.7	0.1	1.1	1.0
Ghana	431.0	498.6	14608.7	23.7	710.0	17.3	9.0	3.0	0.1	0.2	0.2
Yemen, Rep.	416.5	464.6	18032.9	22.2	270.0	12.4	0.7	0.5	0.0	0.0	0.0
Italy	373.1	2063.3	1841086.0	58.9	210.0	59.9	7.0	18.7	0.0	0.2	0.8
Iran, Islamic Rep.	368.1	581.4	228558.2	73.7	1100.0			15.2	0.0	0.7	0.7

Sovereign	Avg. MTe3	Avg. $M	GDP $M	Pop. (1e6s)	Workers (1e3s)	Protein P.C.	Fish Protein	R. value (%)	R. GDP (%)	R. jobs (%)	R. protein (%)
Sierra Leone	296.0	221.4	2047.6	5.6	250.0	14.7	9.9	1.5	0.2	0.2	0.0
Sweden	288.0	224.0	417163.9	9.3	14.0	70.9	8.4	35.9	0.0	0.1	2.0
Kiribati	276.1	549.5	111.3	0.1	25.0	37.5	22.4	50.5	249.4		2.6
Portugal	253.5	546.1	199459.0	10.5	75.0	69.0	15.2	12.2	0.0	0.2	0.4
Algeria	250.0	549.3	114114.6	36.5	170.0	25.0	1.2	5.4	0.0	0.1	0.3
Korea, Dem. Rep.	245.5	204.5		24.4		10.0	2.6	392.3			25.0
Venezuela, RB	236.0	555.7	175846.7	28.6	560.0	45.8	3.1	14.2	0.0	0.6	0.7
Australia	226.7	1155.7	780435.0	21.7	170.0	71.9	5.8	3.6	0.0	0.1	0.2
Oman	209.4	441.2	37617.9	2.9	89.0	45.9	6.9	0.1	0.0	0.0	0.0
Gambia, The	203.4	233.6	722.1	1.6	130.0	17.2	7.9	2.6	0.8	0.6	0.1
Gabon	196.2	250.5	9746.7	1.5	26.0	42.4	9.5	9.8	0.3	0.5	0.9
Micronesia, Fed. Sts.	188.8	391.7	246.1	0.1	42.0	37.5	22.4	22.1	35.3		0.8
Germany	188.4	502.2	3044174.2	81.7	6.4	62.2	4.5	13.8	0.0	0.0	1.5
Greece	184.3	964.6	242794.1	11.1	110.0	61.9	5.3	12.6	0.0	0.3	0.4
Solomon Islands	170.5	375.9	517.5	0.5	19.0	18.7	10.8	5.2	3.8	0.4	0.3
Côte d'Ivoire	167.3	200.9			120.0			2.0			0.1
Egypt, Arab Rep.	162.7	233.7	112422.9	76.8	3300.0	24.5	6.2	5.3	0.0	0.6	0.2
Georgia	160.7	96.6	8140.9	4.4	3.0	26.7	2.3	12.8	0.2	0.0	0.7
Somalia	154.2	268.4		9.4	480.0			1.7		0.3	0.2
Madagascar	152.3	273.6	5744.7	20.5	630.0	10.4	1.5	0.7	0.0	0.0	0.0
Cameroon	145.2	151.4	18897.8	20.1	130.0	13.6	5.2	14.1	0.1	0.2	2.2
Mozambique	145.1	209.9	8649.7	23.4	900.0	6.2	2.4	0.4	0.0	0.0	0.0
Panama	143.2	208.4	22012.1	3.6	23.0	40.9	5.1	0.1	0.0	0.0	0.0
Netherlands	139.2	369.4	718725.8	16.5	8.6	70.8	7.0	26.7	0.0	0.0	2.4
Uruguay	132.7	159.1	21780.6	3.4	5.7	47.7	1.7	60.2	0.4	0.2	3.8
Poland	132.1	114.0	368092.0	38.3	14.0	52.6	5.8	62.8	0.0	0.0	2.8
Tanzania	115.4	203.7	18708.9	43.8	190.0	10.1	2.1	1.7	0.0	0.0	0.3
Tunisia	111.9	199.3	38497.4	10.4	250.0	25.8	3.7	7.8	0.0	0.5	0.3
Finland	109.5	61.1	214677.9	5.3	150.0	69.7	10.2	27.9	0.0	1.6	2.8
Liberia	105.6	156.3	877.9	3.8	150.0	7.4	0.6	1.5	0.3	0.2	0.1
Ukraine	102.2	66.5	93985.5	46.2	41.0	40.2	3.8	19.6	0.0	0.0	1.7
Libya	101.9	225.3	44446.6	5.9	32.0			25.4	0.1	0.4	0.6
Maldives	98.6	191.5	1428.5	0.3	170.0	72.2	52.2	20.7	2.8	20.1	0.9
Latvia	96.1	44.5	17241.7	2.1	19.0	57.7	8.7	37.4	0.1	0.7	2.1
Saudi Arabia	95.1	317.6	419780.2	26.8	40.0	36.2	2.2	5.4	0.0	0.0	0.3
Congo, Rep.	89.2	128.0	7331.3	4.0	22.0			0.8	0.0	0.0	0.0
Croatia	77.8	92.9	47170.6	4.4	16.0	45.9	6.0	9.9	0.0	0.1	0.5
United Arab Emirates	75.9	260.1	207803.5	7.3	52.0	37.7	5.5	0.2	0.0	0.0	0.0
Estonia	75.3	30.3	15075.2	1.3	19.0	51.2	3.9	27.6	0.1	0.8	2.1
Benin	75.2	88.6	5114.4	9.2	300.0	11.8	3.7	7.1	0.1	0.6	1.1
Palau	70.8	158.0	195.2	0.0	4.6			27.3	22.1		1.1
Guyana	68.0	87.9	905.1	0.8	330.0	34.2	8.5	31.0	3.0	36.1	1.0
Suriname	66.5	98.8	2127.2	0.5	250.0	27.8	4.7	26.7	1.2	33.9	1.1
Colombia	66.3	99.6	179103.9	45.8	620.0	32.4	1.8	7.0	0.0	0.2	1.5
Nauru	65.4	139.7			0.4			70.7			3.6
Togo	63.9	83.0	2441.3	6.2	47.0	7.3	1.9	13.5	0.5	0.2	0.7

Sovereign	Avg. MTe3	Avg. $M	GDP $M	Pop. (1e6s)	Workers (1e3s)	Protein P.C.	Fish Protein	R. value (%)	R. GDP (%)	R. jobs (%)	R. protein (%)
Costa Rica	62.2	96.5	24460.5	4.6	13.0	38.1	3.1	7.3	0.0	0.0	0.2
Bahrain	54.6	205.9	19861.1	1.2	150.0			3.2	0.0	0.7	0.2
Dominican Republic	50.8	103.1	43285.6	9.9	740.0	26.2	2.4	0.9	0.0	0.2	0.0
Fiji	43.0	149.2	3126.6	0.9	40.0	32.8	9.7	0.8	0.0	0.1	0.0
Tuvalu	41.5	77.9	24.4	0.0				12.9	41.2		0.6
Marshall Islands	41.1	89.7	146.9	0.1	5.6			9.6	5.9		0.5
Guatemala	41.0	56.8	31899.6	14.0	120.0	18.3	0.4	8.9	0.0	0.2	0.3
Kuwait	39.6	65.6	90492.4	2.8	70.0	51.5	4.0	0.0	0.0	0.0	0.0
Equatorial Guinea	38.4	87.4	9055.6	0.7	32.0			5.0	0.0	0.5	0.2
Nicaragua	37.8	83.9	7210.9	5.8	33.0	20.5	1.5	0.7	0.0	0.0	0.0
Jamaica	34.5	59.8	11075.8	2.7	220.0	36.8	6.7	0.6	0.0	0.1	0.0
El Salvador	34.3	35.3	18409.4	6.2	41.0	22.9	1.9	0.0	0.0	0.0	0.0
Cuba	30.3	68.6	51654.9	11.3	1700.0	29.9	1.6	0.4	0.0	0.1	0.0
French Polynesia	28.0	103.1		0.3		66.1	13.7	0.2			0.0
Congo, Dem. Rep.	25.3	43.9	15179.2	60.6	1500.0	25.3	7.8	0.3	0.0	0.0	0.0
Haiti	25.2	42.9	4467.9	9.8	700.0	10.3	1.5	7.3	0.1	1.2	0.3
Cabo Verde	23.5	58.5	1239.2	0.5	92.0	34.9	3.5	0.2	0.0	0.1	0.0
Lithuania	22.7	13.8	29114.0	3.1	8.2	75.5	16.6	59.3	0.0	0.3	2.6
Trinidad & Tobago	21.1	49.3	18693.6	1.3	200.0	38.1	5.7	2.3	0.0	0.7	0.1
Brunei Darussalam	21.1	31.6	9916.2	0.4	6.6	46.7	5.5	1.6	0.0	0.1	0.1
Bahamas, The	20.6	125.1	7763.5	0.4	63.0	53.6	7.2	7.4	0.1	2.3	1.0
Vanuatu	19.1	30.5	478.9	0.2	24.0	28.2	10.1	1.6	0.1	0.4	0.1
Comoros	18.9	29.3	409.1	0.7	160.0			23.9	1.7	22.5	1.2
Bulgaria	18.5	21.0	33358.2	7.5	12.0	39.2	2.0	14.2	0.0	0.0	0.2
Mauritius	18.2	50.8	7505.6	1.3	23.0	39.7	6.8	0.2	0.0	0.0	0.0
Qatar	18.1	80.5	89058.6	1.5	19.0			0.4	0.0	0.0	0.0
Honduras	17.1	48.6	11357.9	7.5	78.0	25.4	0.8	3.2	0.0	0.1	0.3
Samoa	16.2	30.7	494.1	0.2	13.0	48.4	12.4	2.3	0.1	0.8	0.1
Kenya	15.9	40.3	23035.1	39.9	51.0	17.1	1.3	0.2	0.0	0.0	0.0
Sao Tome & Principe	15.1	33.5	159.7	0.2	47.0	16.6	7.9	10.0	2.1	8.5	0.5
Hong Kong SAR, China	12.0	14.7	214007.3	7.0	19.0			0.0	0.0	0.0	0.0
Seychelles	11.0	16.8	1126.1	0.1	6.9			0.5	0.0		0.0
Eritrea	10.3	12.7	1110.9	5.6	55.0			0.3	0.0	0.0	0.0
American Samoa	7.9	20.1		0.1				1.0			0.0
Lebanon	7.9	15.4	27488.3	4.3	79.0	30.5	2.7	7.5	0.0	0.4	0.4
Tonga	7.1	12.2	265.8	0.1	14.0			1.2	0.1	0.4	0.1
Belgium	7.1	27.8	408788.6	10.8	2.1	58.7	6.3	44.4	0.0	0.0	2.9
Belize	6.9	11.3	1240.0	0.3	23.0	27.6	3.7	6.0	0.1	1.0	0.3
Iraq	6.7	19.1	65294.8	30.3		12.2	0.8	0.0	0.0		0.0
Syrian Arab Republic	6.2	12.9	30396.7	20.7	17.0			16.0	0.0	0.0	0.9
Timor-Leste	6.2	10.9	648.4	1.1		16.4	1.1	2.9	0.0		0.3
Singapore	5.5	6.9	164366.5	4.9	33.0			4.0	0.0	0.0	0.1
Israel	5.0	15.7	169857.9	7.5	5.8	72.2	4.5	0.0	0.0	0.0	0.0
Barbados	4.9	5.6	4071.0	0.3	42.0	51.4	11.8	7.8	0.0	2.2	0.2
Gaza Strip	4.9	11.3						0.0	0.0	0.0	0.0
Albania	4.6	6.9	10126.0	2.9	19.0	51.2	1.8	18.3	0.0	0.3	0.3

Sovereign	Avg. MTe3	Avg. $M	GDP $M	Pop. (1e6s)	Workers (1e3s)	Protein P.C.	Fish Protein	R. value (%)	R. GDP (%)	R. jobs (%)	R. protein (%)
Cyprus	4.2	15.1	18518.1	1.1	2.2	47.4	6.2	22.1	0.0	0.1	0.7
Antigua & Barbuda	3.9	12.5	1085.4	0.1	11.0	59.3	13.3	0.0	0.0		0.0
Malta	3.6	13.1	6558.4	0.4	5.0	59.2	8.2	26.6	0.1	0.8	1.2
Djibouti	3.4	7.3	866.7	0.8	3.5	12.1	0.6	0.0	0.0	0.0	0.0
St. Vincent	2.9	8.9	595.5	0.1	10.0	50.1	5.6	24.0	0.4	4.4	1.7
Sudan	2.9	6.6	31923.4	34.8	38.0			0.0	0.0	0.0	0.0
Grenada	2.7	5.0	680.9	0.1	13.0	42.7	10.0	18.6	0.1		1.0
St. Lucia	2.2	3.9	1022.5	0.2	18.0	51.6	8.8	26.4	0.1	5.4	1.1
Romania	1.8	4.7	114387.0	20.5	73.0	49.2	1.7	37.3	0.0	0.3	1.7
St. Kitts & Nevis	1.6	6.9	577.3	0.1	6.7	48.0	9.9	7.5	0.1		0.4
Dominica	1.6	4.4	422.6	0.1	10.0	46.5	8.1	39.8	0.4		2.2
Montenegro	1.4	2.8	2720.4	0.6		58.5	2.9	27.9	0.0		0.7
Slovenia	0.8	2.0	39327.9	2.0		55.6	2.9	0.0	0.0		0.0
Jordan	0.3	0.5	16027.3	5.9	0.3	29.6	1.7	0.0	0.0	0.0	0.0
Bosnia & Herzegovina	0.1	0.1	12437.3	3.9		31.3	1.6	0.0	0.0		0.0

Table S7 Summary of the calculated risk measures by sovereign country. The first 7 columns report key attributes of the countries, which are inputs to the risk measure calculations. These are, in order, the total catch (in 1000 mtons) averaged over 2005 - 2014; total landed value (in millions of 2010 USD) averaged over 2005 - 2014; the GDP (in millions of 2010 USD); the population (in millions); the total workers in fisheries (in thousands); the average protein per capita (g/capita/day); and the protein per capita from fish (g/capita/day). The final four columns are our main risk measures, as described in the text. These are the % of fishery landed value at risk, the % of GDP at risk; the % of jobs at risk; and the % of food risk.

SM 3.5 Empirics

To empirically validate our model and evaluate the impacts of international shocks, we analyzed cross-country connections in the RAM Legacy Stock Assessment Database (*43*). We identified stocks for which we could evaluate how recruitment in one country related to spawning biomass fluctuations in another. The RAM database contains stock assessments for 343 stocks across 12 countries. Of these, there are 58 instances where the same stock is assessed in multiple countries, including 21 cases where the stock was assessed within an individual country and by a multinational organization.

Not all of these instances report recruitment. We identified 93 recruitment time series, across 47 species, which can be related to biomass timeseries from at least one other country. Since biomass and recruitment are assessed differently in different regions and reported in different units, we analyzed the extent to which the variance in stock fluctuations explain cross-boundary fluctuations in recruitment.

For each species and country combination, we performed the regression

$$r_{it} = \alpha + \sum_j \left(\beta_{1j} x_{jt} + \beta_{2j} x_{j,t-1}\right) + \epsilon_{it}$$

where r_{it} is the recruitment in region i in year t, and it is explained by spawning stock levels from the recruitment year, x_{jt}, and the year before it, $x_{j,t-1}$, in each available country (including $j = i$, the country of recruitment). Recruitment values in the RAM database are reported with lags, so that r_{it} represents the recruitment from the spawning biomass x_{jt}, with the same year index, even though the spawning stock biomass for a given recruitment is often from a previous year. Stock predictors for which the coefficient is negative were dropped and the regression was re-run.

Our goal in performing this regression was not to provide a full explanation of the drivers of recruitment. The statistical relationship above is only useful to relate the total amount of variation that is explanable by variation in local and remote stock levels. We perform an ANOVA on the regression results and sum over the portion of variance explained by local (β_{1i} and β_{2i}) and cross-boundary (β_{1j} and β_{2j} for $j \neq i$) stocks. This allowed us to produce a rough estimate of the extent to which stocks are dependent or otherwise connected.

Table S8 shows correlations between the fraction of variance explained by local or cross-boundary stocks and other attributes of the stocks. In the first set of columns, labeled "Self-Supply", the correlation was taken between the fraction of variance explained bu local stocks or cross-boundary stocks and an indicator for whether the variance in question describes self-supply (that is, the effect of a stock level on its own recruitment). These columns aimed to validate our resilience measure, which we adopted from Fishbase. Resilience measures the capacity of a stock to recover from a shock, and is based on the intrinsic growth rates and fecundity information. Stocks with high resilience are expected to be able to recover best from spawning biomass losses.

In our results, high resilience stocks showed a much higher correlation, followed by medium resilience, and followed by low resilience, implying that for high resilience stocks, shocks in other countries tend to have little explanatory power for variation in recruitment. This relationship is shown in figure S10.

Next, we correlated our cross-boundary dependence measure against the fraction of variance explained by the corresponding stocks. In the correlation, the portion attributable to the local EEZ is associated with the local stock variance explained, and the portion attributable to other EEZs is associated with the sum of other stock variance explained portions. The dependence measure used is the portion of the total catch from each country. Across all RAM stocks, the correlation is 0.15 (and insignificant), suggesting poor predictive ability of our measure to

Resilience	Self-Supply	95% CI	Dependence	95% CI
All RAM	0.36	0.21 - 0.49	0.15	-0.09 - 0.37
High Resilience	0.53	0.27 - 0.72	0.07	-0.35 - 0.46
Medium Resilience	0.40	0.13 - 0.62	0.10	-0.37 - 0.53
Low Resilience	0.21	-0.03 - 0.42	0.24	-0.16 - 0.57

Table S8 Correlations between the fraction of variance explained and either an indicator of self-supply or the simulated dependence measure. The self-supply indicator (left) validates our resilience measure, with high resilience stocks showing low responsiveness to shocks in other countries. The correlation with the dependence measure (right) is correspondingly higher for medium and low resilience stocks.

explain shocks. However, the weakest predictability comes from high resilience stocks, while medium and low resilience stocks show higher correlations.

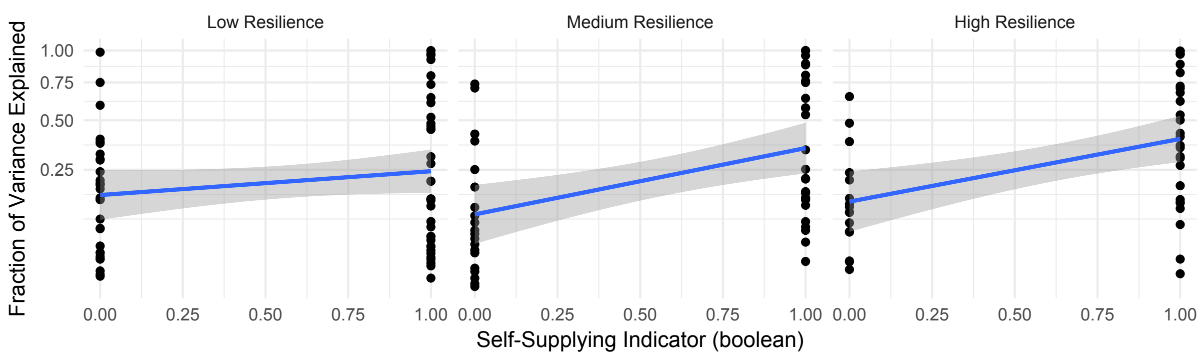

Fig. S10 Fraction of variance explained to each observation of spawning stock, split by self-supply. Each observation is identified as representing self-supply or foreign supply. As resilience increases, self-supply stocks dominate the variance explained.

The confidence intervals across all of these results are wide, due to the small number of observations, but the results support a number of aspects of this work. First, resilience is a key criteria, where variations in non-recruitment-limited stocks within the RAM database are not well explained by our metric.

Second, for stocks with lower resilience, our dependence measure can predict the extent to which countries support recruitment internally and for other countries.

Third, variation in recruitment appears to be explained by the stock levels in countries outside of the spawn drift flows that we measure (where simulated flow is 0). This suggests additional long-distance or cascading effects. In 25 of 70 cases, the simulated flow between the RAM countries is 0, but the fraction of variance explained is on average 28%.

SM 3.6 Sensitivity analyses

SM 3.6.1 Results for 1995 – 2004

The results in the main paper applied flows to a baseline of catches from 2005 – 2014. In the absence of strong management, stocks are subject to considerable variability, and some are experiencing long-term decline. The decade-long average used in the paper represents approximate recent catches, removing some forms of variability. As a sensitivity analysis, we related estimated flows to a baseline of catches from 1995 – 2004, to see how longer-term fishery changes affect our results. We also applied 1995 - 2014 averages for sovereign-level baseline values for GDP, populations, and labor force, but kept all other values unchanged, including the flow climatology. For convenience, we refer to the 1995 – 2004 baseline as the 2000 baseline, and the 2005 – 2014 baseline as the 2010 baseline.

Figure S11 shows the imports and exports for the 2000 baseline. The ranking of countries by their catch attributable to spawn imports is different, but the collection of countries that are in the top 7 remain unchanged. Two notable changes are a large decrease in imported value for Japan from 2000 to 2010, and a increase in value imported of low-resilience species for Indonesia. Similarly, the 8 EEZs with the most exported catch remain unchanged between 2000 and 2010, although they are reordered. The greatest difference between 2010 and 2000 values in exported catch is in Alaska, which exported catch more than doubles.

The socioeconomic risks corresponding to figure 4 in the main paper for the 2000 baseline are

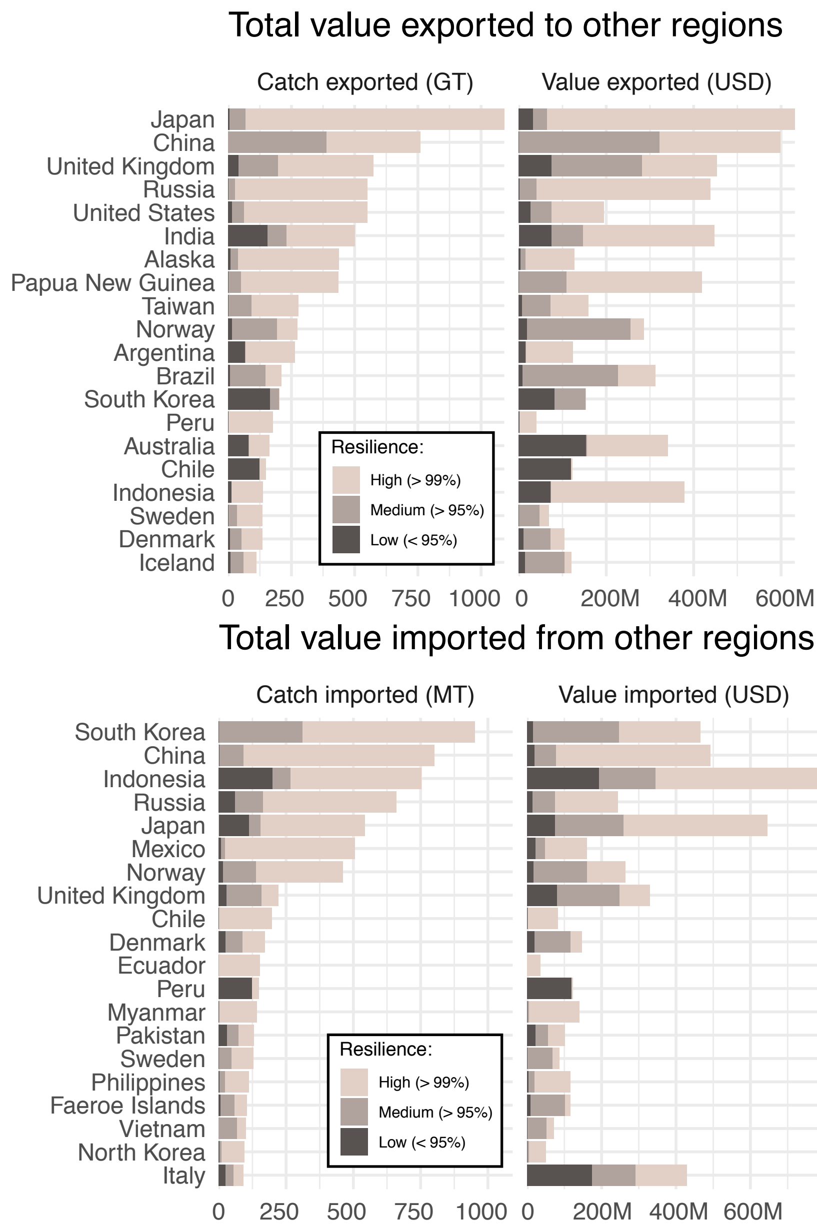

Fig. S11 Result corresponding to figure 3 in the main text for a 1995 - 2004 baseline. Top: Top 20 countries sorted by total outflowing catch (mtons) and value (USD). **Bottom:** Top 20 countries sorted by total inflow of catch (mtons) and value (USD) at risk. 1995 - 2004 values of catch and landed values are used, attributing them to larvae by species. Resilience levels represent the estimated decline a population can endure without being considered vulnerable to extinction.

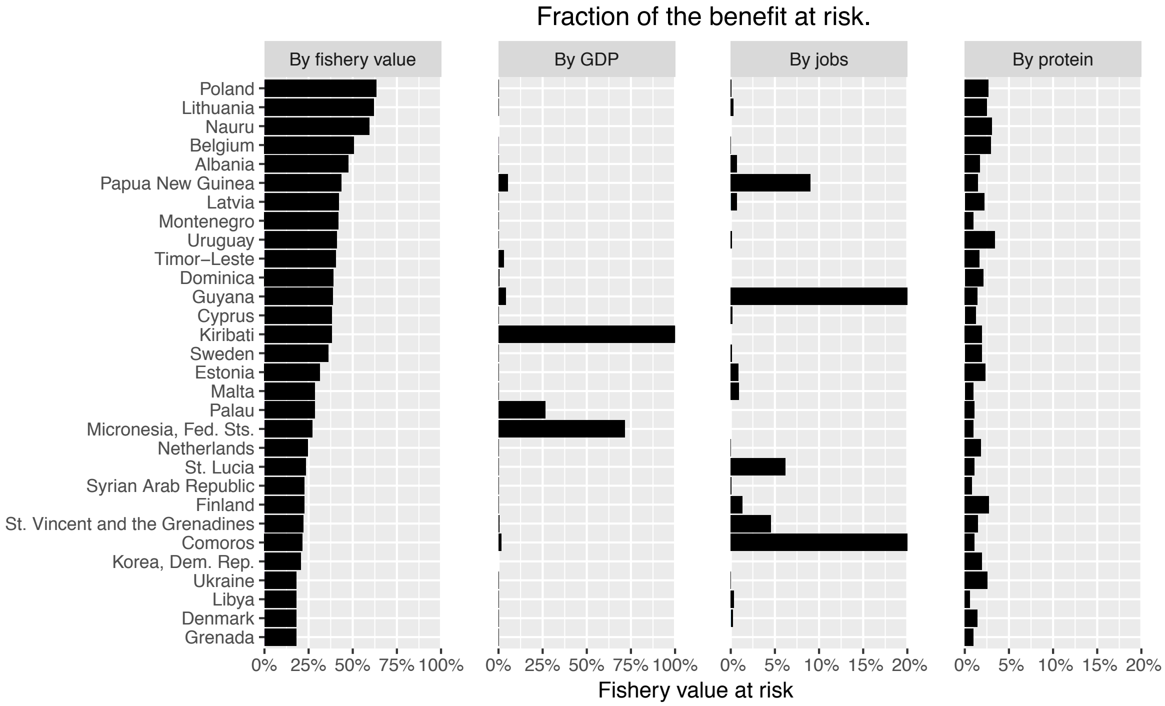

Fig. S12 Results corresponding to SI figure S9. Normalized values of well-being at risk, for the top 30 country's as ranked by the portion of their fishery sector at risk. *By fishery value* is the value at risk divided by the country's total landed value, averaged over the last 10 years. *By GDP* is the value at risk divided by the country's GDP, as a measure of the entire economy at risk. *By Jobs* takes the values in the *By fishery value* column and multiplies them by the portion of the population involved in direct and indirect fisheries work. *By protein* is an index of the risk in needed fishery protein for health.

shown in figure S12. In this case, there are greater changes and shifts. This is because the regions most at proportional risk tend to be smaller countries.

SM 3.6.2 Annual variability

Our main results are based on a climatology of ocean currents. This climatology removes eddies and annual variability that may be an important driver of connectivity.

In order to examine the influence of climate variability on EEZ connectivity, three years of data were selected for our simulations based on climatic conditions. The years were chosen based on

El Niño-Southern Oscillation (ENSO) and North Atlantic Oscillation (NAO) indices, as these are two dominant modes of variability that can significantly alter ocean surface velocities. The years used were the following:

1. July 2005 to June 2006 – Neutral year
2. July 2007 to June 2008 – La Nina, positive NAO
3. July 2009 to June 2010 – El Niño, negative NAO

Both ENSO events and NAO peak in the boreal winter (December to February). In order to capture the full development of these events continuously over the end of the calendar year, we began with the July before the event and ended with the following June.

We then determined transition matrices for each year individually, and only average them together when computing import and export attributable to catch. These results are shown in figure S13. The results are very similar, with the top 8 exporting countries and the top 4 importing countries appearing in the same order and with very similar magnitudes. We also found that the network of flows in this case retains the small-world property, with a weighted small-coefficient of 1233.5.

SM 3.6.3 Reduced mobility analysis

The estimates for species-specific larval floating duration are very uncertain, and the average distance traveled may be significantly shorter because of larval mortality. To provide a sensitivity test, we reduced the duration under which each species is subject to floating by 30%. This version of the network retains the small-world property, with a weighted small-coefficient of 381.3.

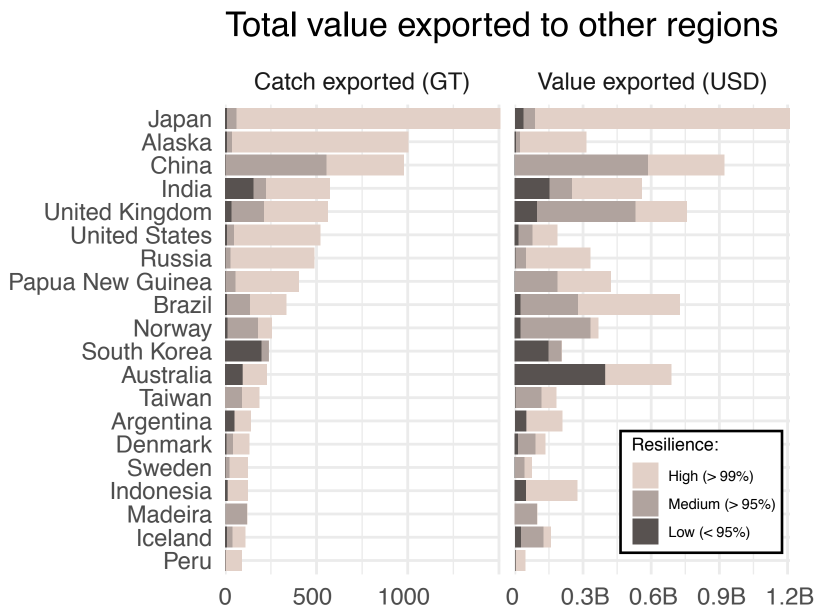

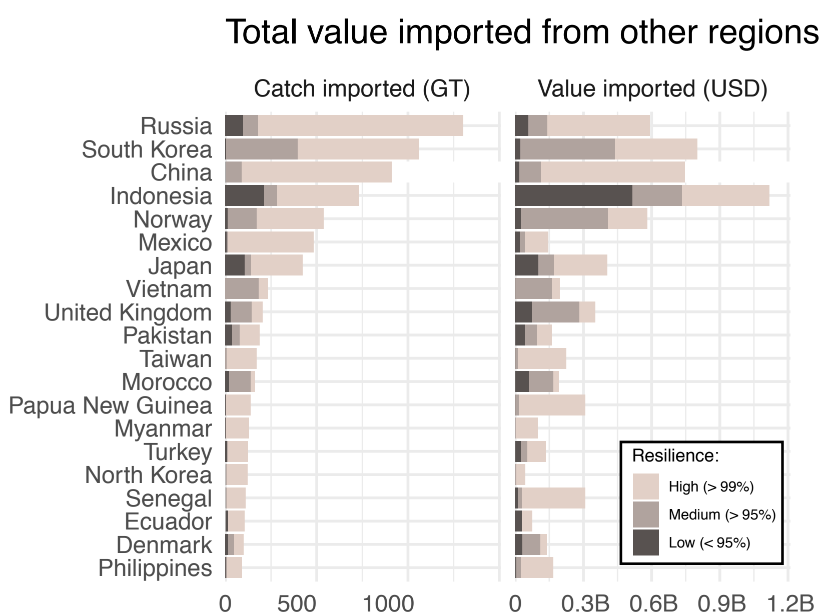

Fig. S13 Result corresponding to figure 3 in the main text, when accounting for annual variability. Top: Top 20 countries sorted by total outflowing catch (mtons) and value (USD). **Bottom:** Top 20 countries sorted by total inflow of catch (mtons) and value (USD) at risk. 1995 - 2004 values of catch and landed values are used, attributing them to larvae by species. Resilience levels represent the estimated decline a population can endure without being considered vulnerable to extinction.

SM 3.6.4 Adult return movement analysis

Many species return to the region they were spawned. In the analysis in the main paper, we assumed that fish recruit and are caught in the EEZ they float to. Here, we assumed that there is some amount of return movement. The net affect of this return movement is that 50% of the fish spawned in region i which drift to region j will return to region i before being caught.

We implemented this by using a new set of species-specific transition matrices

$$(T_k')_{ij} = \begin{cases} 0.5(T_k)_{ij} & \text{if } i \neq j \\ (T_k)_{ij} + 0.5 & \text{if } i = j \text{ and } \sum_m s_{ikm} > 0 \\ 0 & \text{otherwise} \end{cases}$$

In this case, the weighted small-coefficient of the network becomes 1157.